Superconductors in magnetic fields: vortex pinning and relevance to rf applications

Enrico Silva

Dipartimento di Ingegneria Industriale, Elettronica e Meccanica

enrico.silva@uniroma3.it

Microwave group and collaborations

Enrico Silva

Kostiantyn Torokhtii, Andrea Alimenti, Nicola Pompeo

Collaborations

Outline

1 **Superconductors, microwaves and vortex motion**

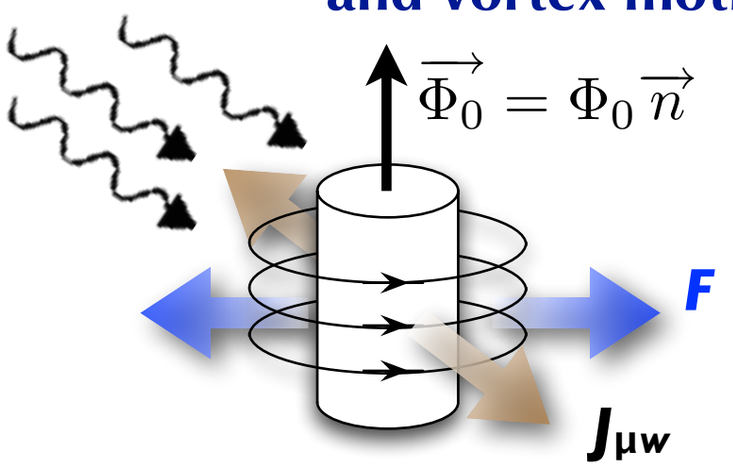

2  **What can we learn**

3 **Experimental techniques**

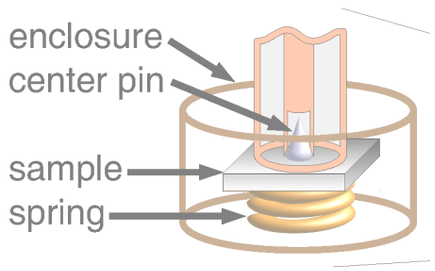

4 **Results (a partial overview)**

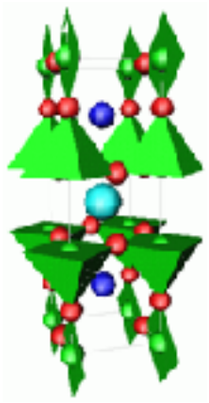

$YBa_2Cu_3O_{7-\delta}$ + second phases

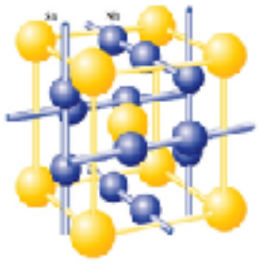

FeSeTe

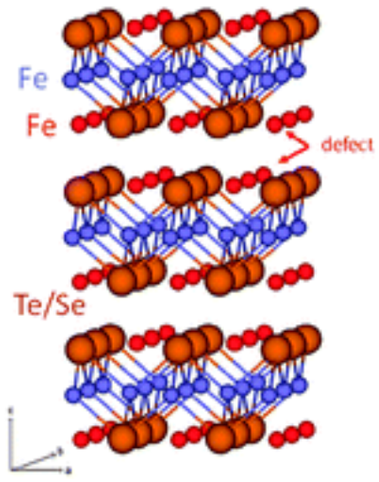

5 **Perspectives for rf in high magnetic fields**

Superconductors

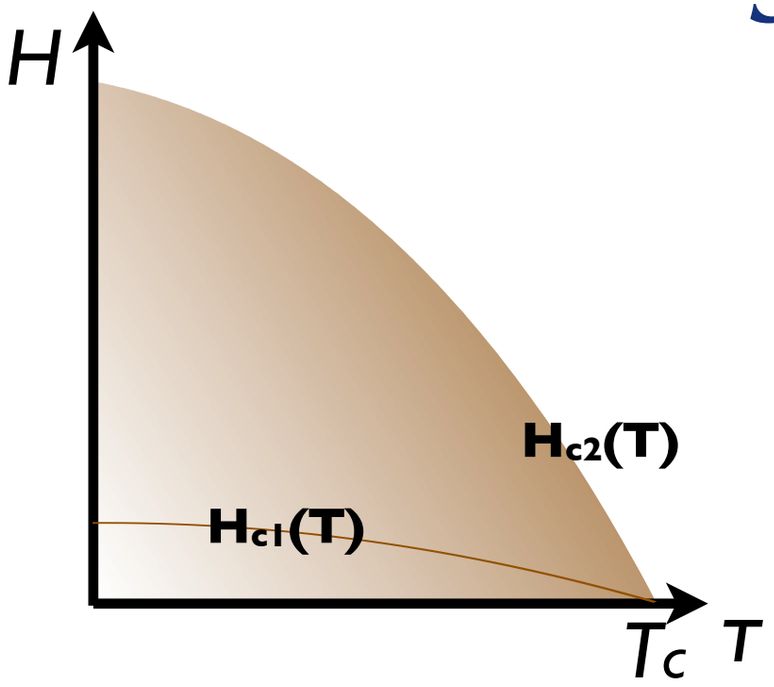

Type-II superconductors

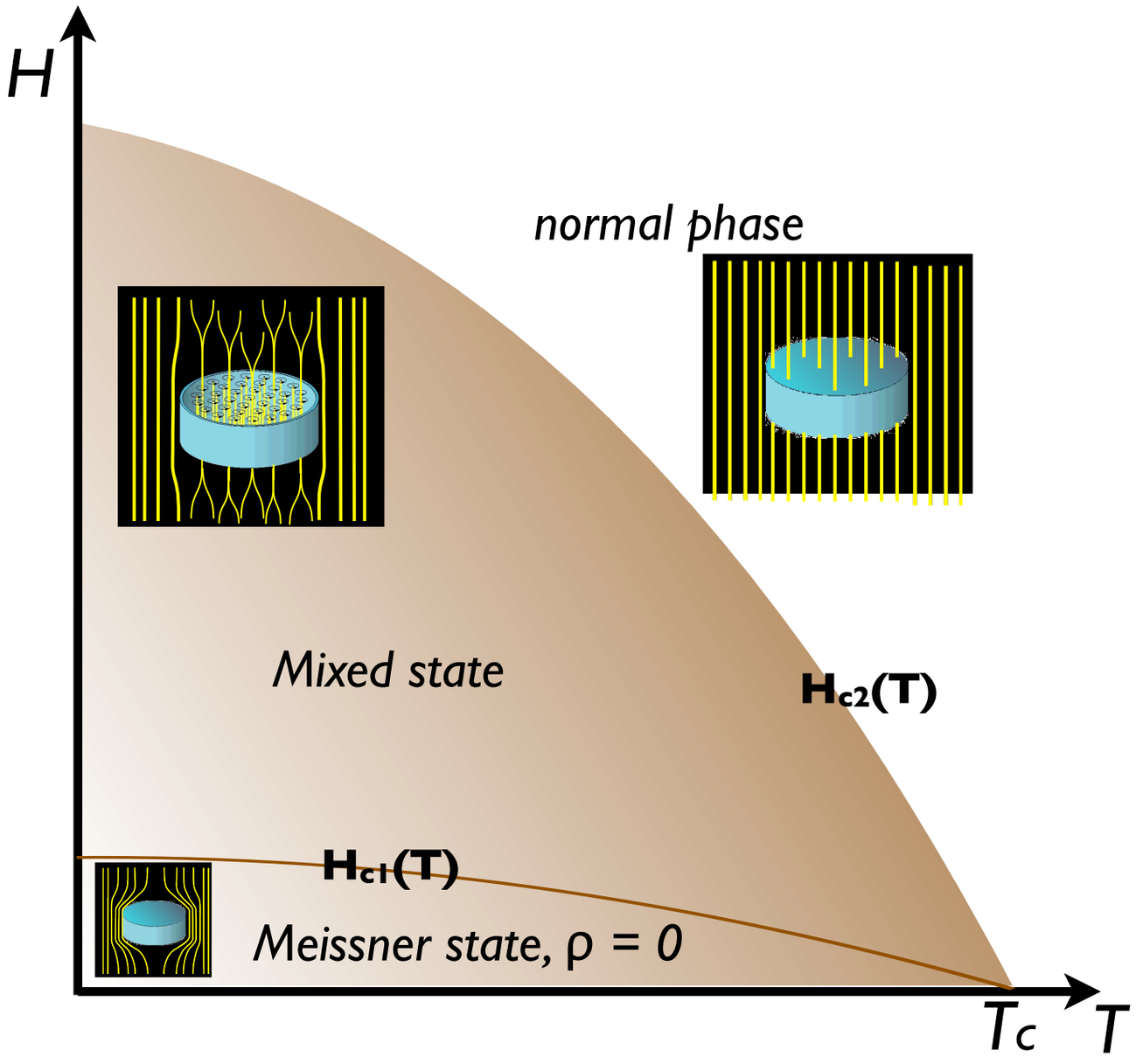

Three regions:

- Meissner state, $H < H_{c1}(T)$
- Mixed state, $H_{c1}(T) < H < H_{c2}(T)$
- Normal state, $H_{c2}(T) < H$

Mixed state, $H_{c1}(T) < H < H_{c2}(T)$:

- Partial penetration of the flux
- Flux quanta ("fluxons", "vortices")
- "Vortex lattice"

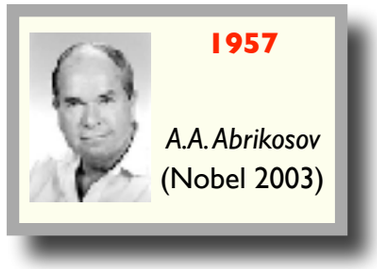

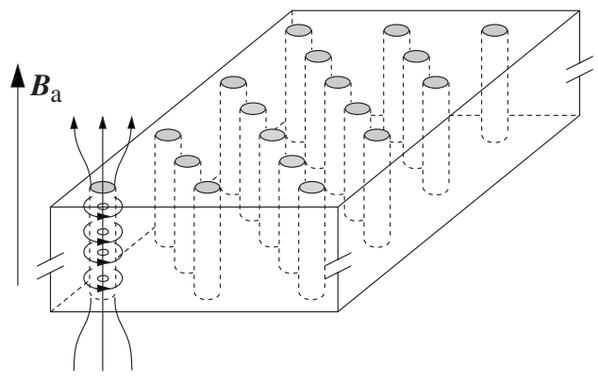

Fluxons / Vortices

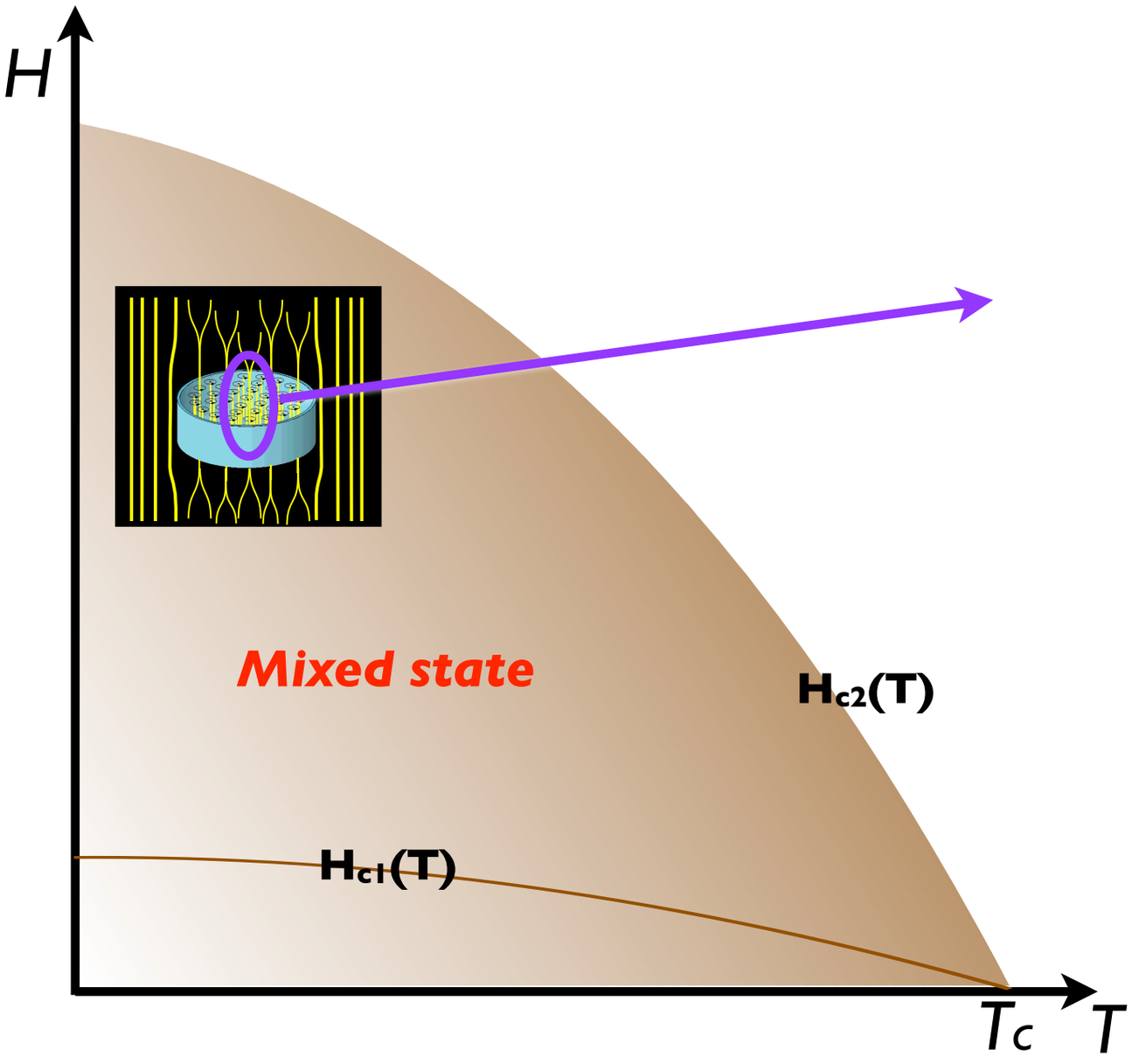

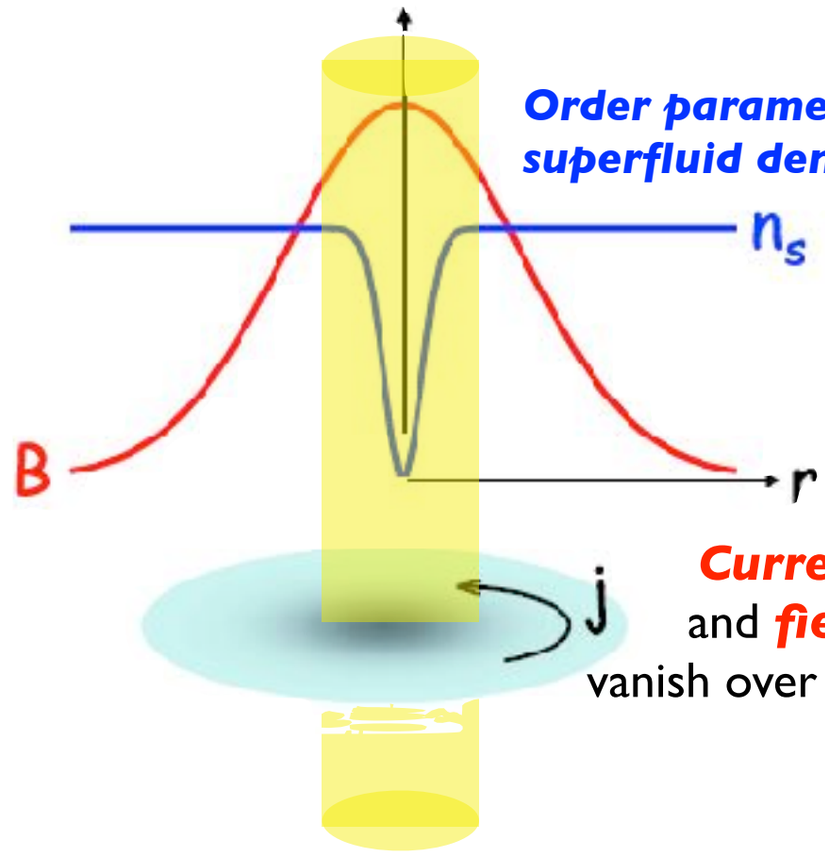

Currents and ***fields*** vanish over ~ λ

"normal" *core* ~ ξ

Flux enclosed:
$\Phi_0 = h/2e$

Moving vortices

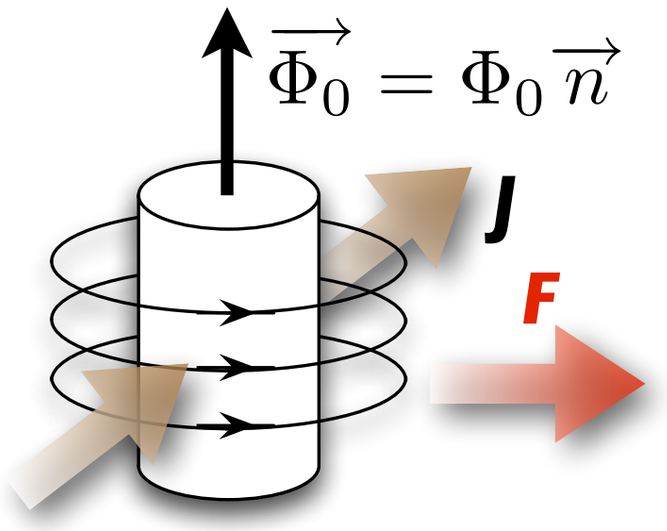

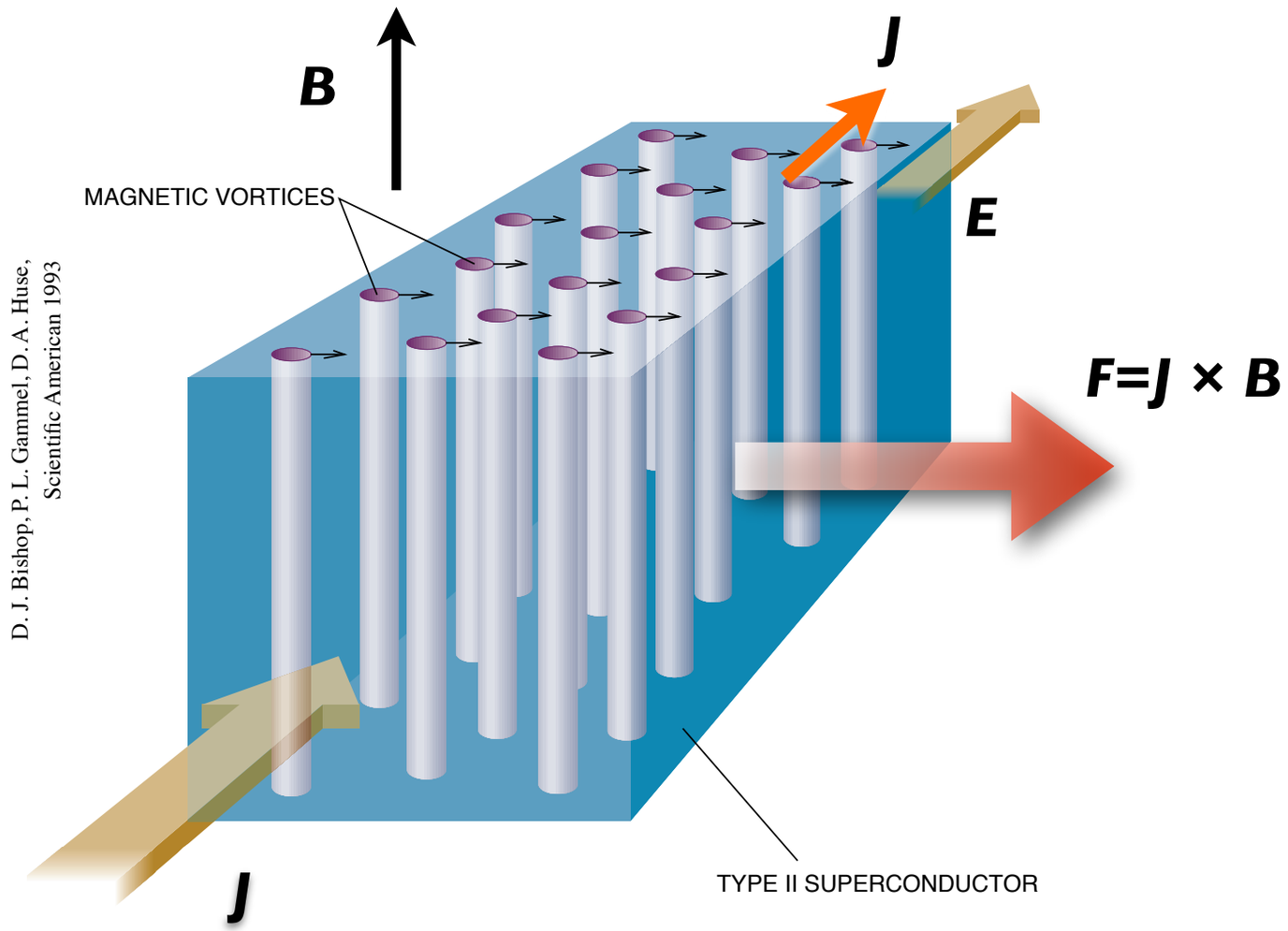

applied **J**

⇓

F (per unit length) on fluxons

⇓

vortices move

⇓

electric field **E**

⇓

emf

⇓

dc: Resistance ≠ 0

ac: Impedance ≠0

⇓

Measurable response

free motion: "flux–flow"

Ideal type-II superconductors

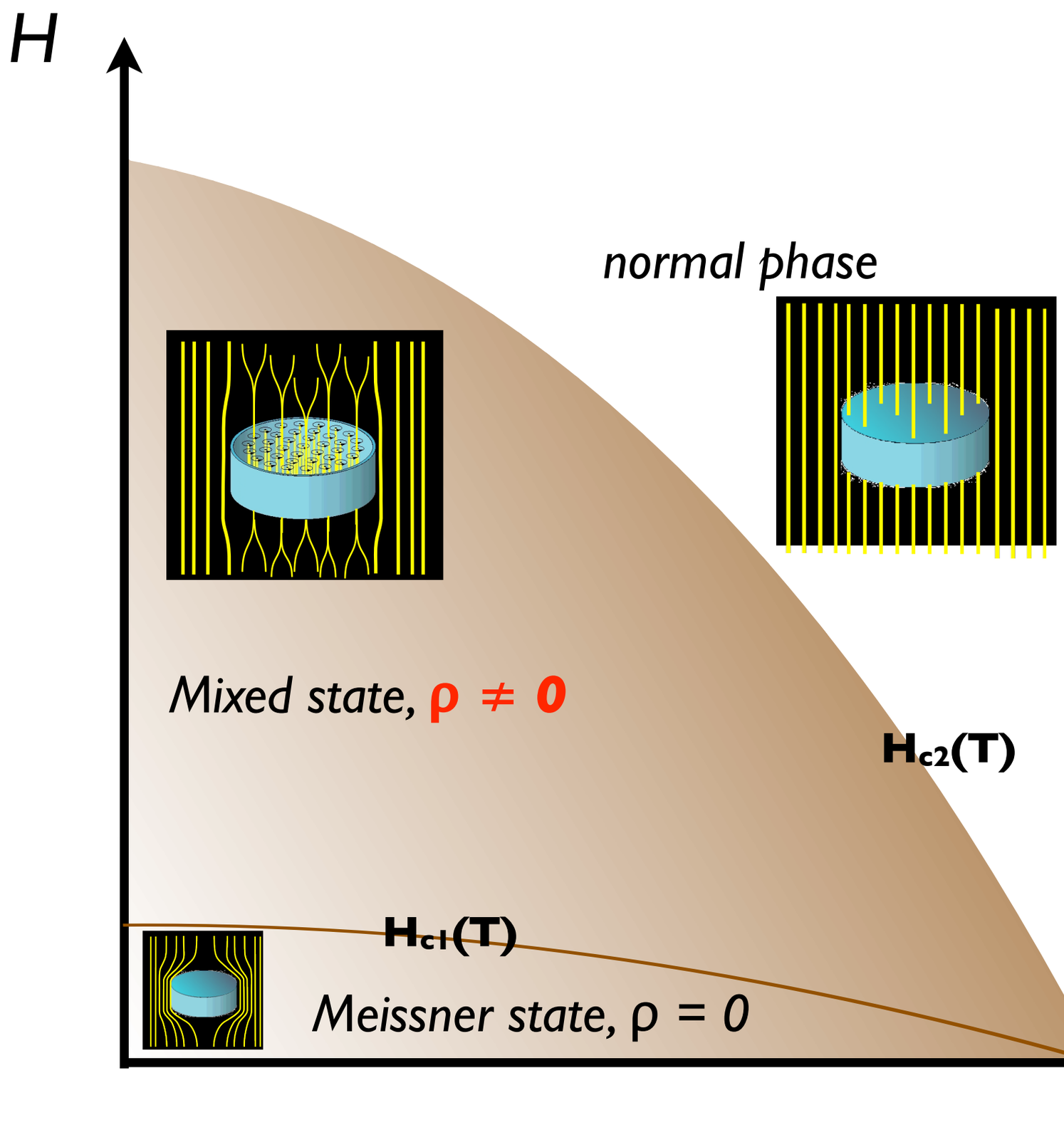

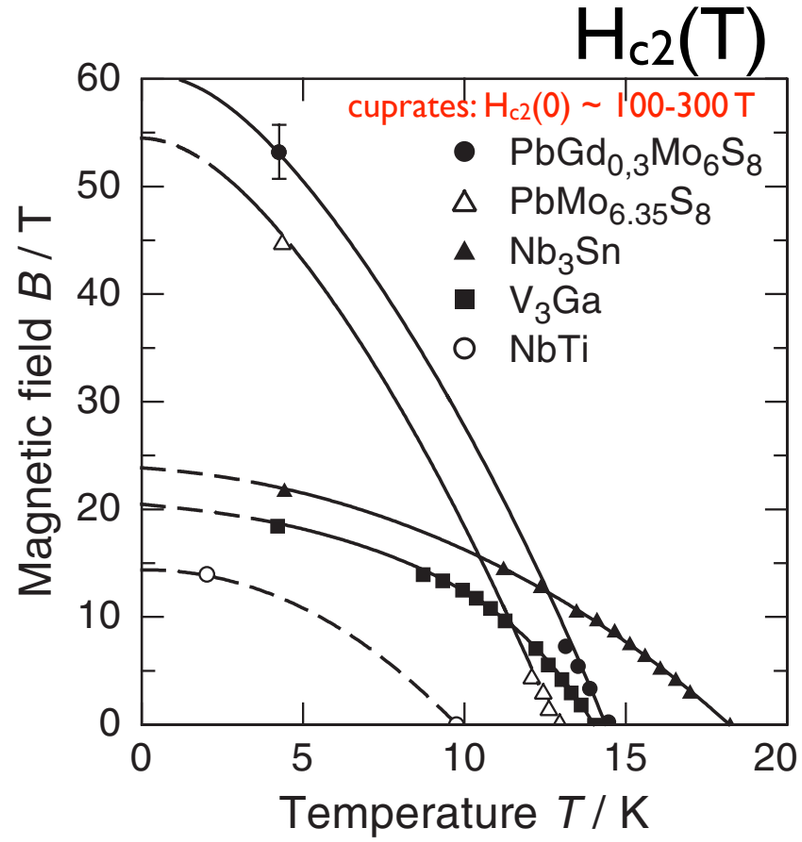

An ideal type-II SC is *resistive* in the mixed state!

... but the normal phase is reached at large/huge fields.

⇒ worth some work!

Stop the fluxons!

Moving fluxons: dissipation → hinder fluxon motion: "pinning"

"suitable" defects: preferential sites for the normal cores

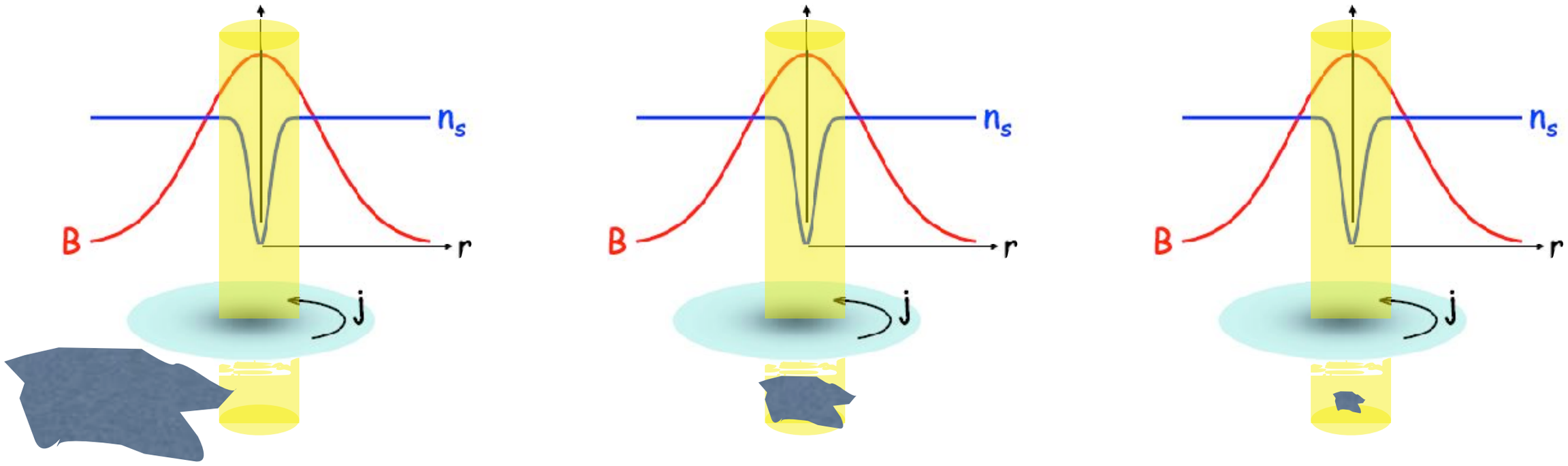

too large: size >>ξ

efficient: size ~ξ

too small: size << ξ

ξ: "magic size" for defects

Stop the fluxons: nanosize matters!

hinder fluxon motion:
"pinning"

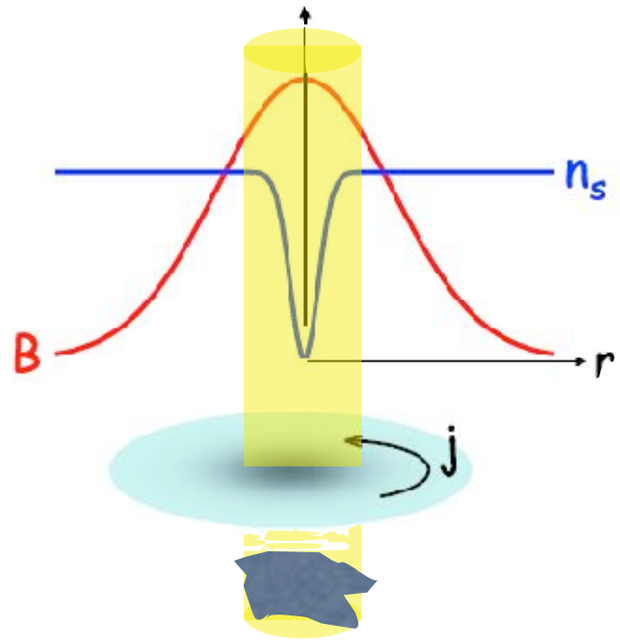

ξ:"magic size" for defects

superconductor	ξ (nm)
Nb	39
Nb_3Sn	3
MgB_2	35-40
$YBa_2Cu_3O_{7-x}$	1.5 (ab plane) 0.3 (c axis)

Here comes nanoscience!

Note: add defects, reduce (maybe to 0) the resistance!
(metals: quite the opposite)

Stop the fluxons: shape matters!

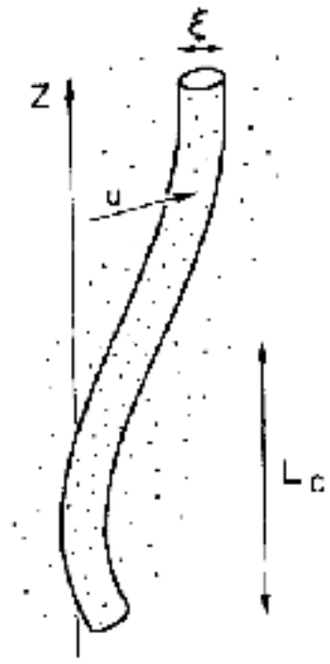

Fluxons can be flexible (energy balance between pinning and vortex elasticity)
⇒ shape of the defects is essential

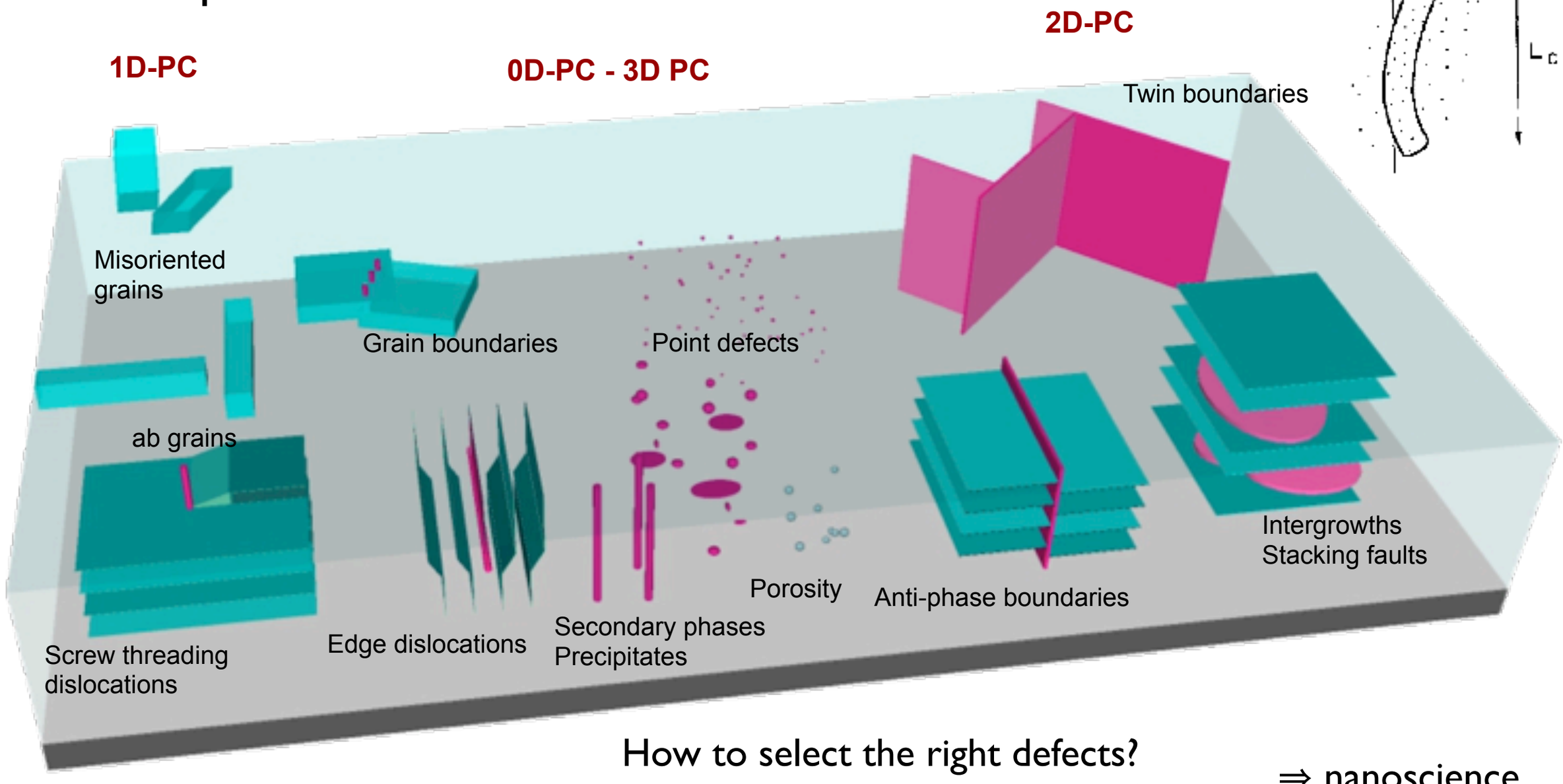

How to select the right defects?
How to insert into the material?

⇒ nanoscience

Pinned fluxons and critical current density

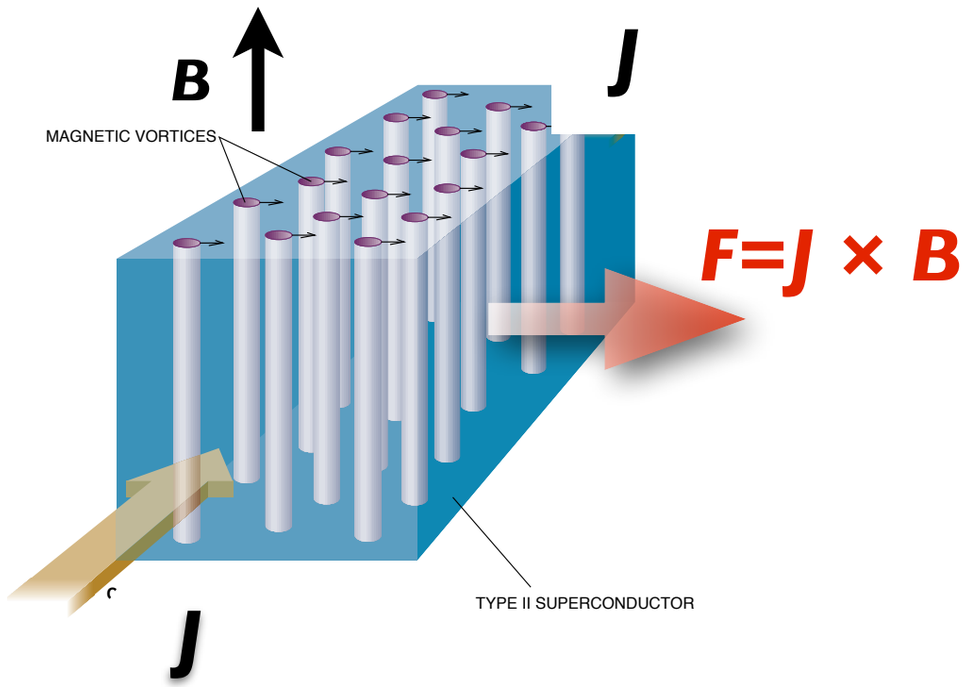

Fluxons stay pinned until the pinning force F_p exceeds J × B

Critical current density J_c:
defined as the onset of dissipation (ill-defined)

J_c: The quantity to maximize

I–V curves

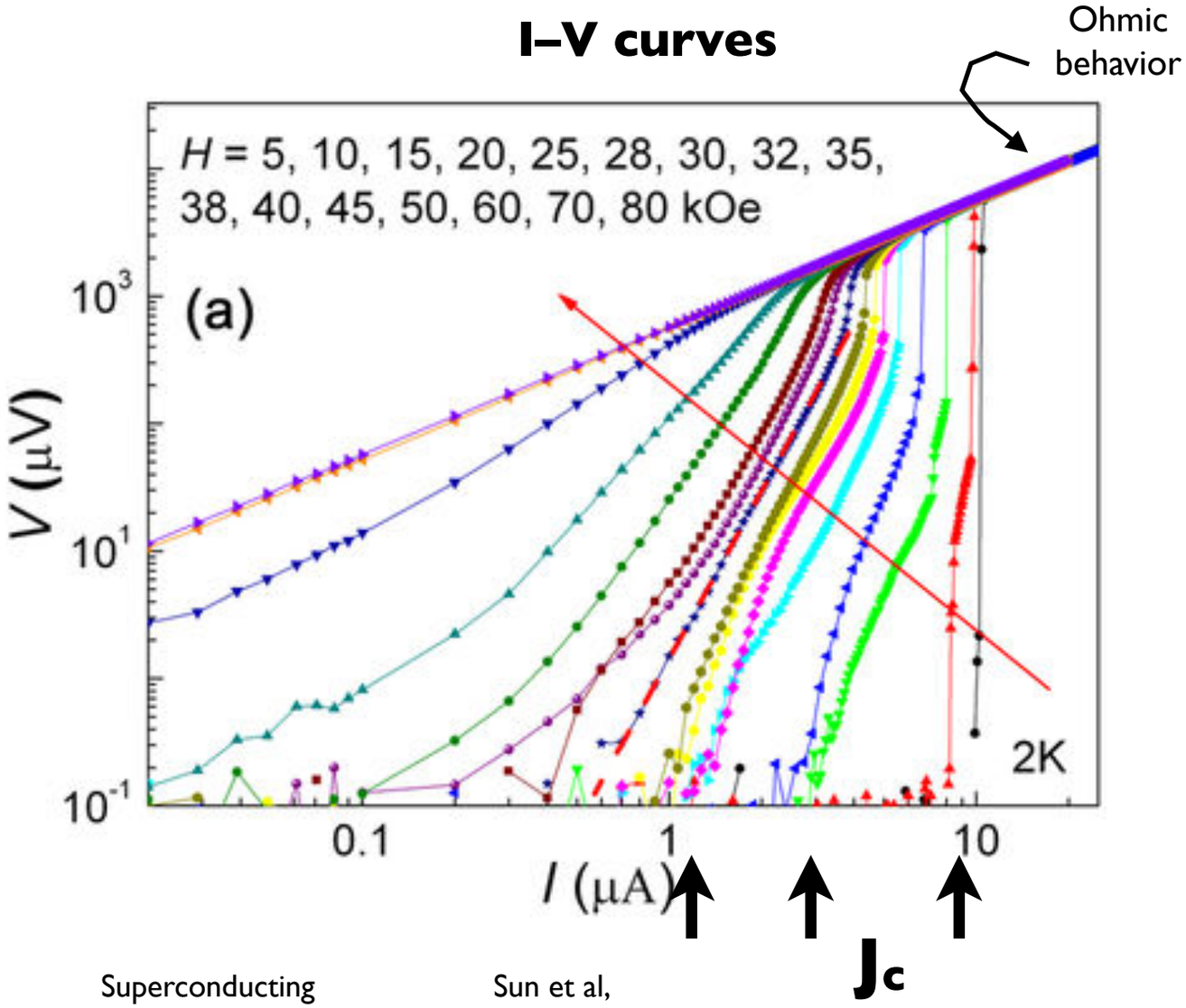

Superconducting W strips

Sun et al, Sci. Rep. 3, 2307 (2013)

"pinned" type-II superconductors

"irreversibility line": below $H_{irr}(T)$, $\rho \approx 0$

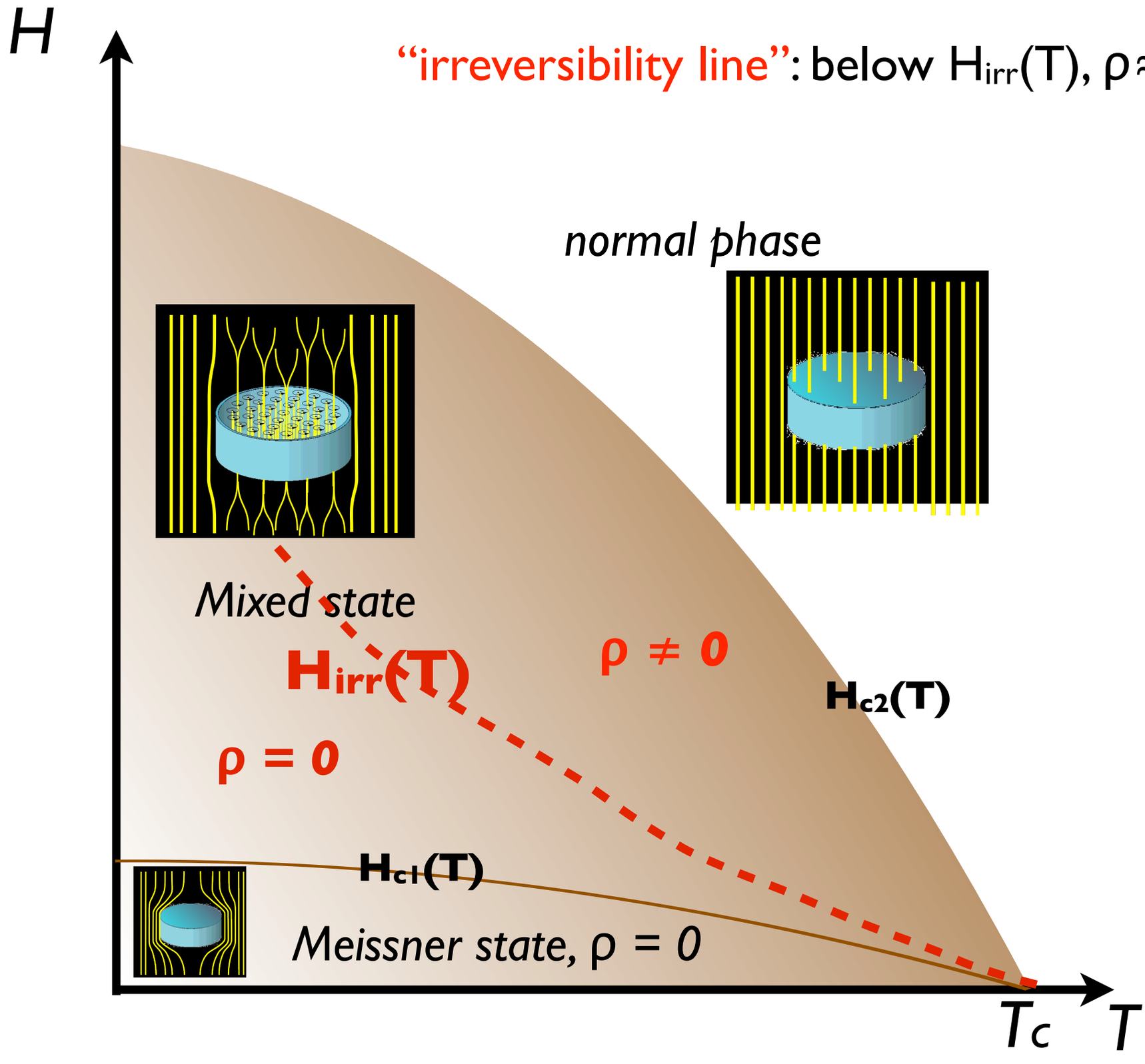

This is a "dc" picture !

The main applications

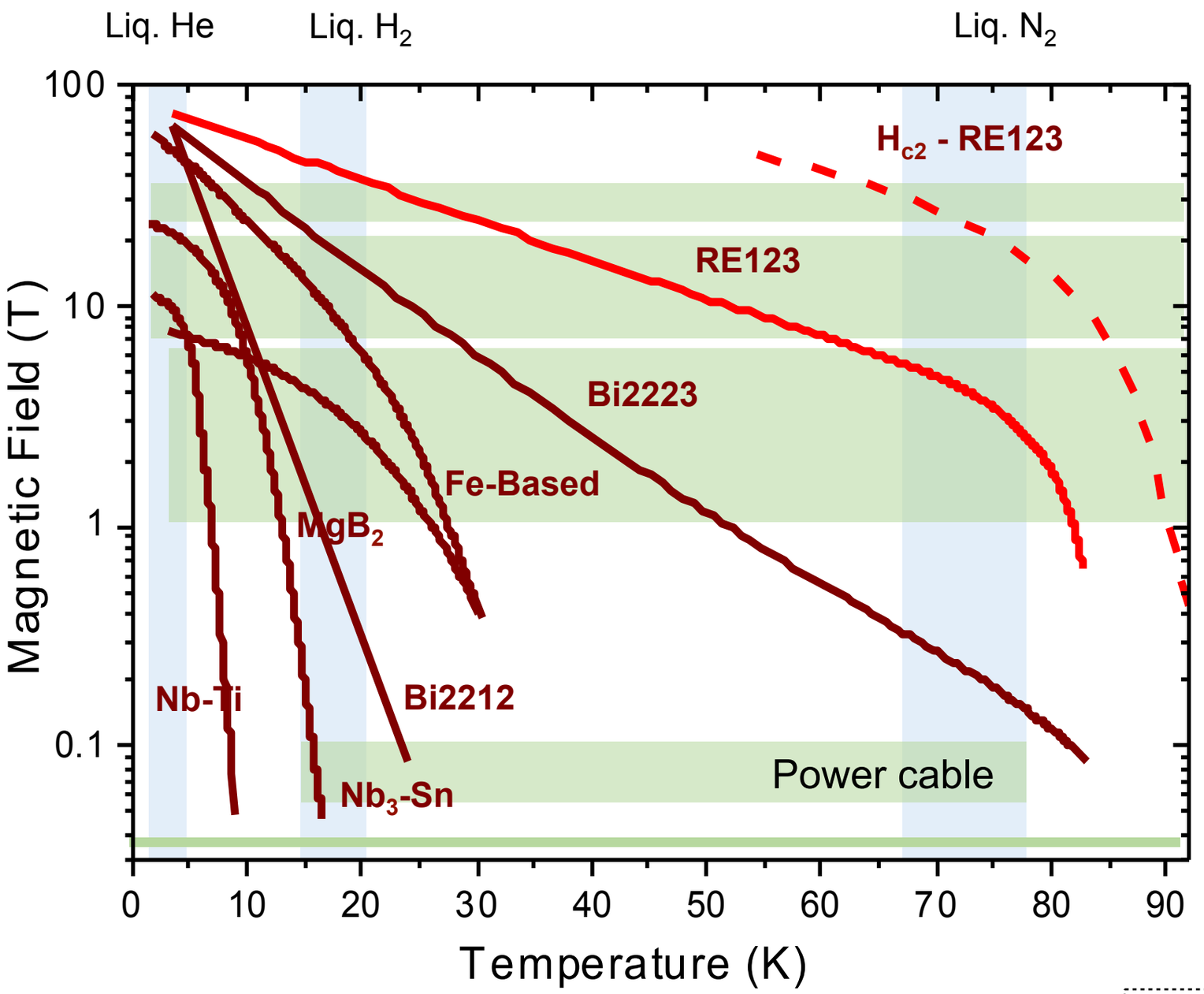

>1GHz NMR

Fusion Accelerator (present)

MAGLEV train, MRI, Magnetic separation

Electronic devices

Applications requiring $J_e > 10^4$ A cm² for various superconducting tapes and wires [Shimoyama, SUST 27 (2014)]

1. stay below the irreversibility line
2. obtain a LARGE J_e

J_e:"engineering current density", critical current Ic divided the section of the *wire* (which includes materials other than the SC alone)

"path to pinning"

superconductor	ξ (nm)	structure
Nb	39	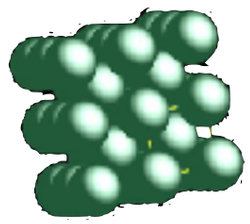
Nb_3Sn	3	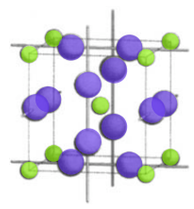
$YBa_2Cu_3O_{7-x}$	1.5 (ab plane) 0.3 (c axis)	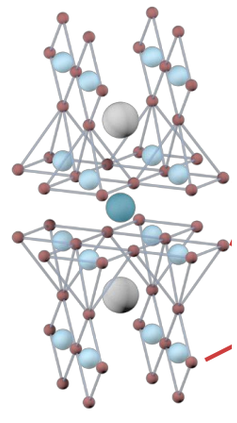

Isotropic materials
Low T (little thermal energy)
⇒ no extreme defect engineering

⇒ Metallurgy

(somewhat sophisticated for Nb_3Sn)

Strongly anisotropic material
High T (large thermal energy)

?

2004: the breakthrough

Strongly enhanced current densities in superconducting coated conductors of $YBa_2Cu_3O_{7-x} + BaZrO_3$

J. L. MACMANUS-DRISCOLL[1*†], S. R. FOLTYN, Q. X. JIA, H. WANG, A. SERQUIS, L. CIVALE, B. MAIOROV, M. E. HAWLEY, M. P. MALEY AND D. E. PETERSON

nature materials | VOL 3 | JULY 2004 |

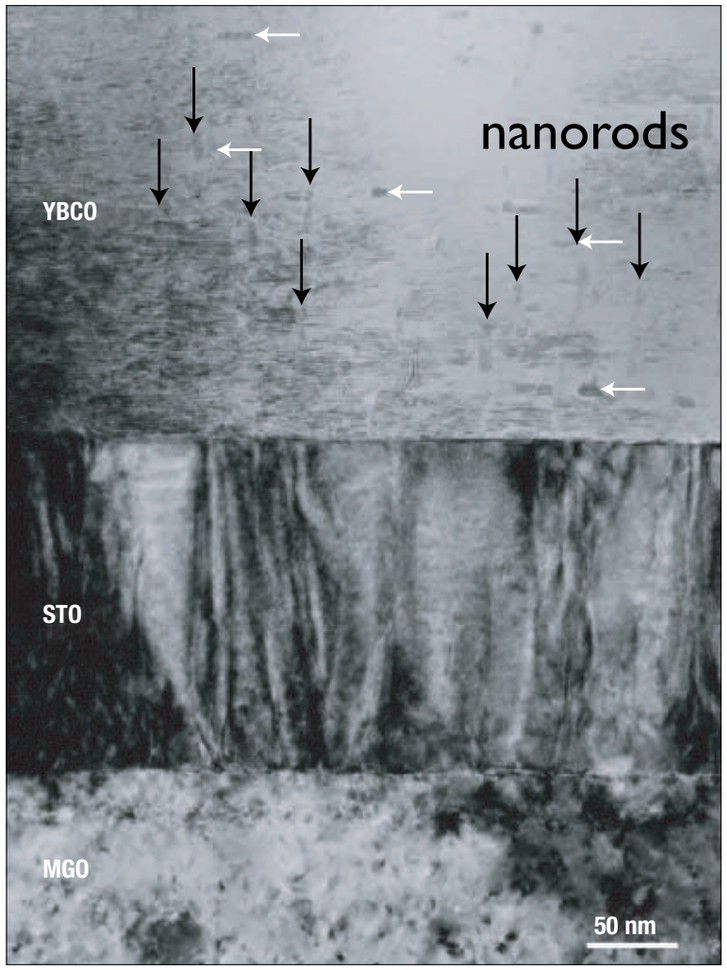

$BaZrO_3$ cubic second phase inserted in the YBCO matrix as *nanorods*, dia. ~5nm

(Cambridge)

Successful insertion of nanorods in YBCO (pulsed laser technique)

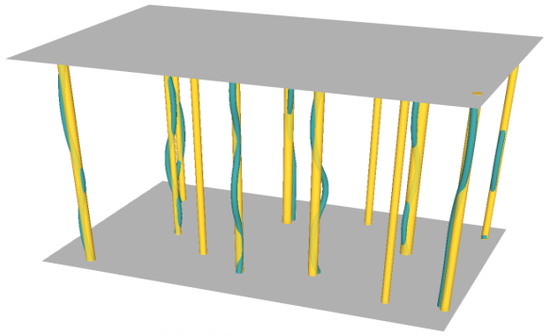

$J_c(H=0)=10^6$ A/cm²!

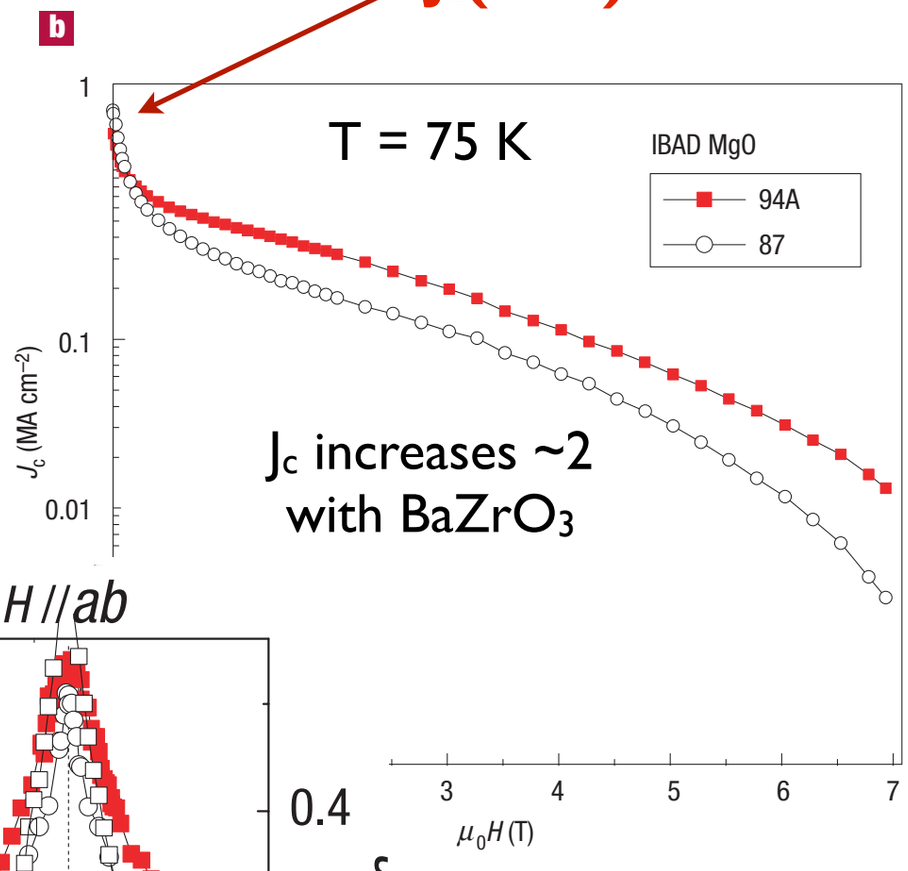

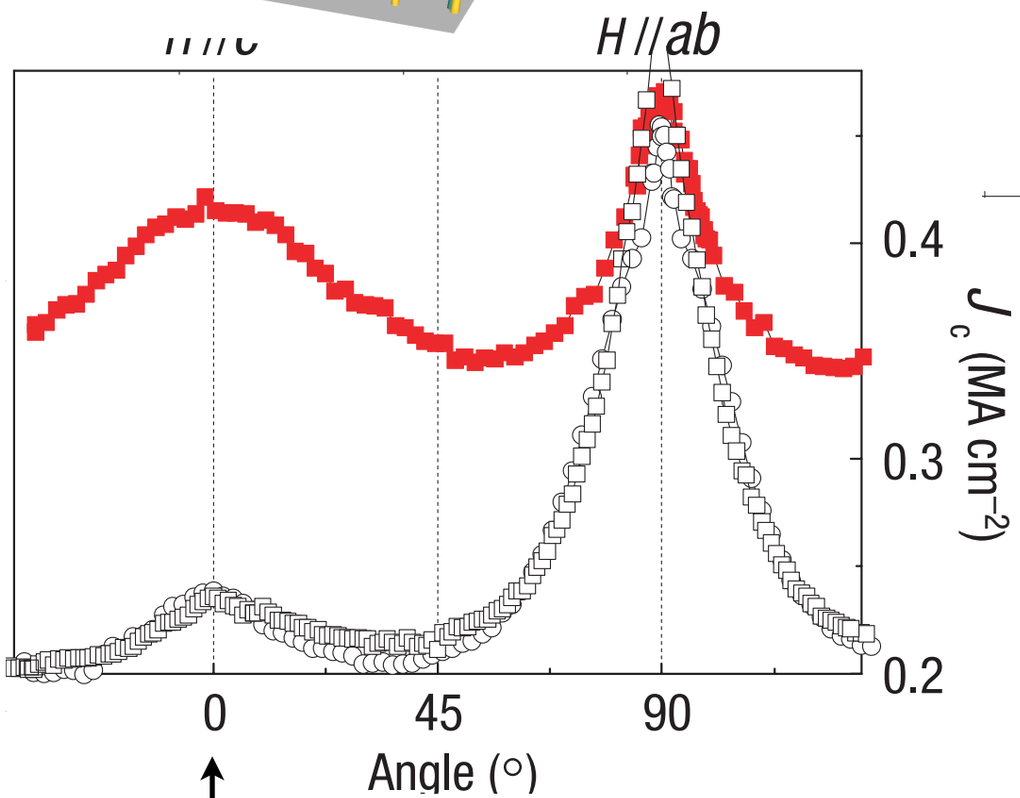

J_c increases when the field is aligned with $BaZrO_3$ nanorods

2007: isotropic pinning

Strong isotropic flux pinning in solution-derived $YBa_2Cu_3O_{7-x}$ nanocomposite superconductor films

J. GUTIÉRREZ*, A. LLORDÉS*, J. GÁZQUEZ, M. GIBERT, N. ROMÀ, S. RICART, A. POMAR, F. SANDIUMENGE, N. MESTRES, T. PUIG AND X. OBRADORS†

nature materials | VOL 6 | MAY 2007

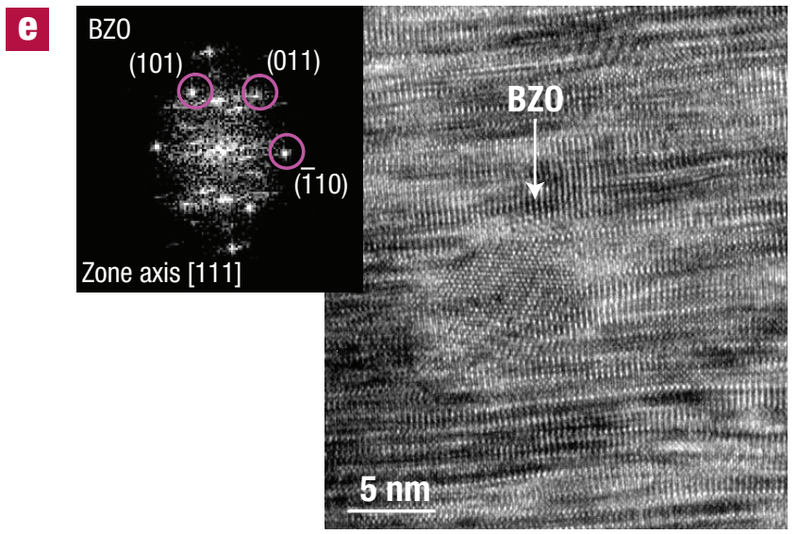

HRTEM:
$BaZrO_3$ cubic second phase inserted in the YBCO matrix as *nanoparticle*, dia. ~7nm

(Barcelona)

Successful insertion of nanoparticles in YBCO (chemical deposition technique)

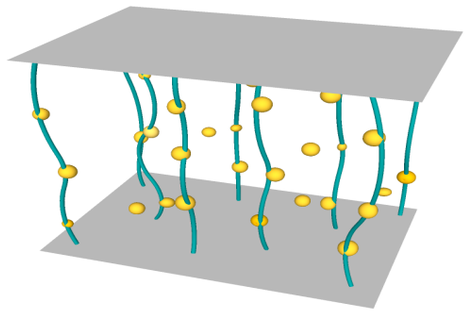

$J_c(H=0)>10^7$ A/cm²!

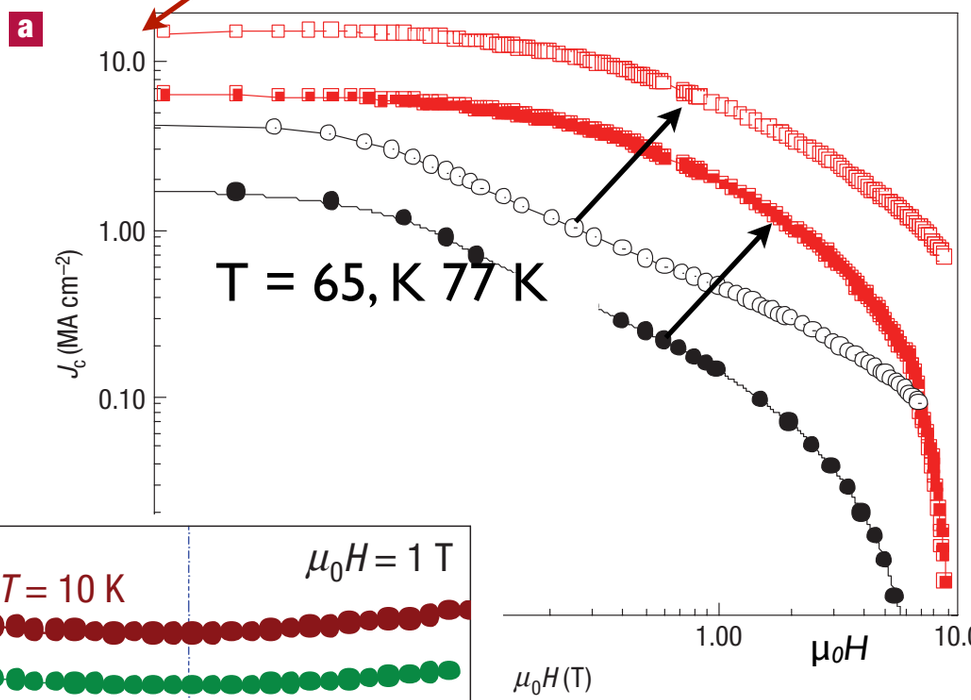

J_c increases ~4 with $BaZrO_3$

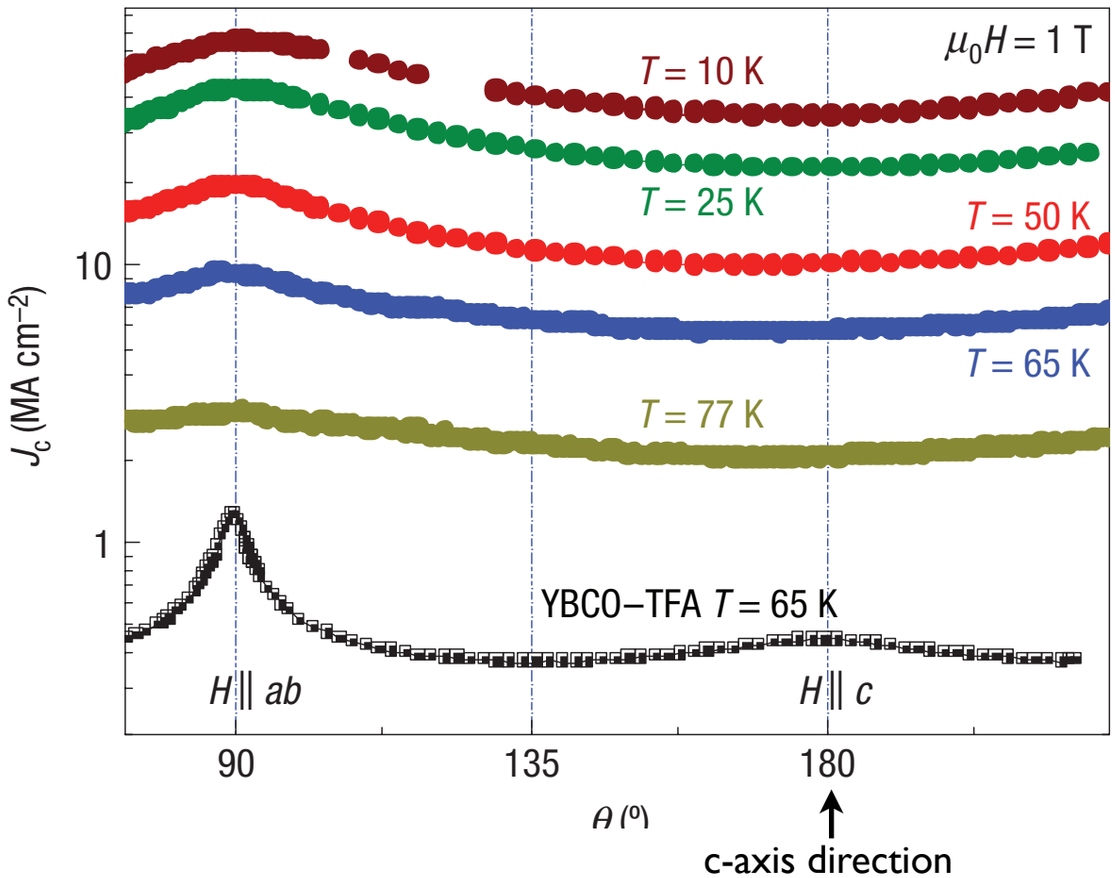

J_c with $BaZrO_3$ nanoparticles *flatter* than in pristine: good for applications

2009: mixed defect shape

Synergetic combination of different types of defect to optimize pinning landscape using $BaZrO_3$-doped $YBa_2Cu_3O_7$

B. Maiorov★, S. A. Baily†, H. Zhou†, O. Ugurlu‡, J. A. Kennison, P. C. Dowden, T. G. Holesinger, S. R. Foltyn and L. Civale

NATURE MATERIALS | VOL 8 | MAY 2009

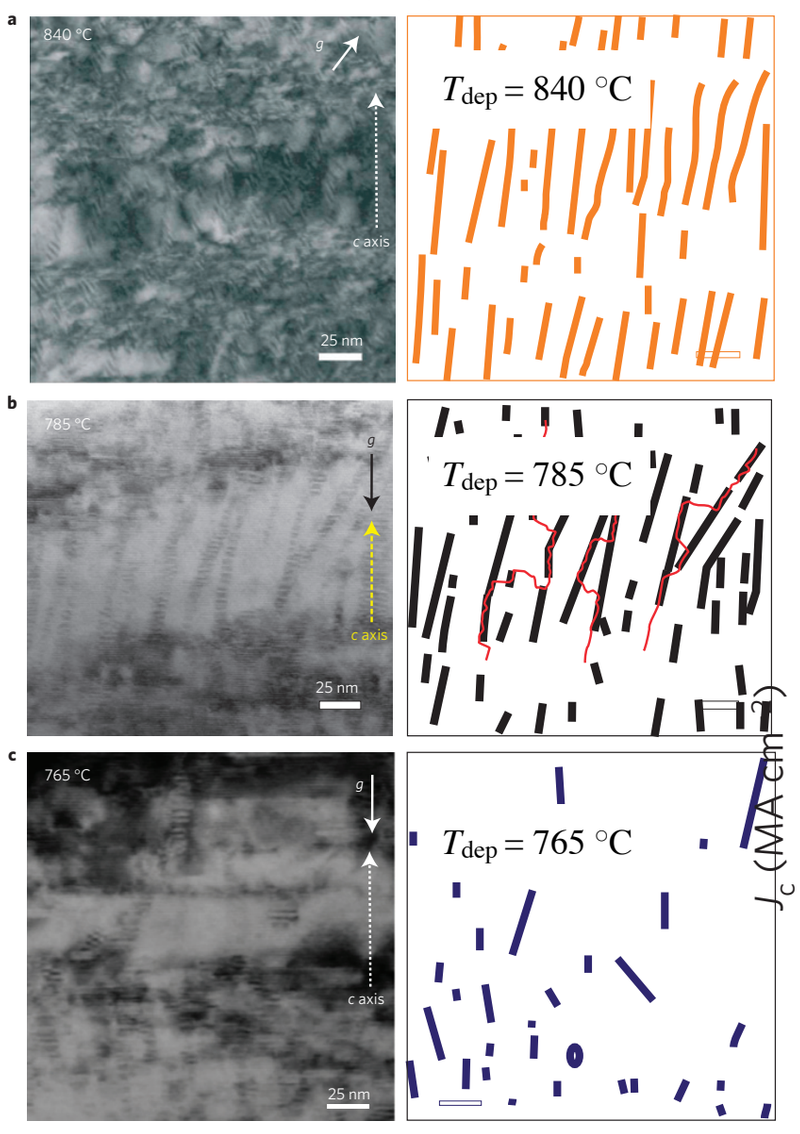

(Los Alamos)

Successful insertion of splayed nanorods in YBCO + nanoparticles (pulsed laser technique). Splay of nanorods + nanoparticles favors efficient pinning (fluxons are flexibles!)

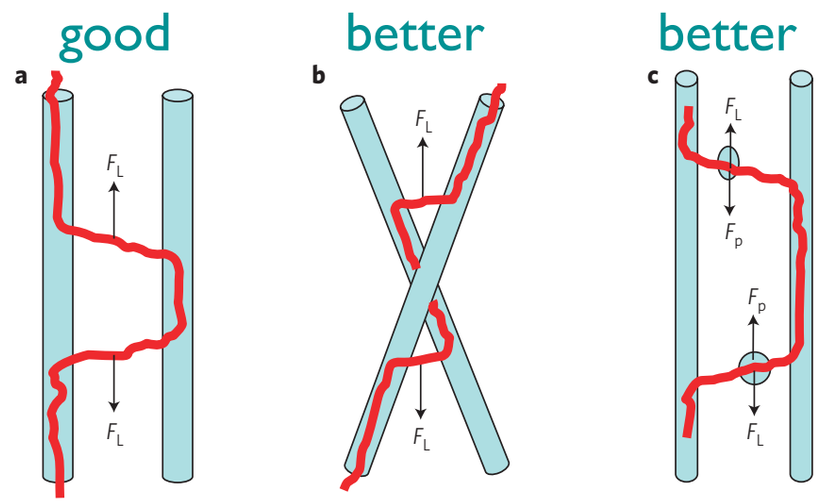

Figure 5 | Diagrams of expansion of vortex double kinks for configurations involving different defects. a, Diagram of two parallel

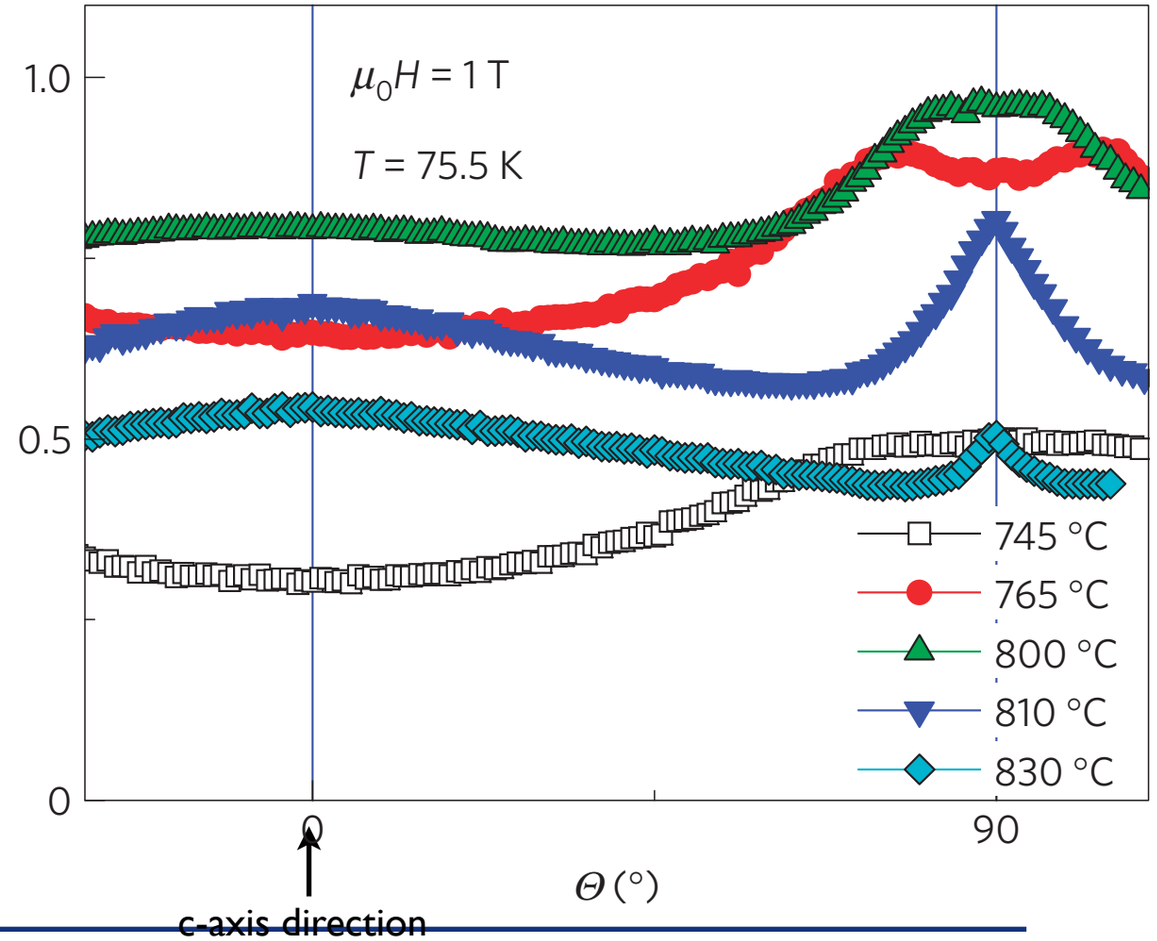

TEM:

$BaZrO_3$ *nanorods + nanoparticle*

Splay depending on deposition T

Engineering nanodefects shape and landscape

2015: heavy second phases doping

(Houston)

APPLIED PHYSICS LETTERS **106**, 032601 (2015)

High critical currents in heavily doped (Gd,Y)$Ba_2Cu_3O_x$ superconductor tapes

V. Selvamanickam,[1,a)] M. Heydari Gharahcheshmeh,[1] A. Xu,[1] E. Galstyan,[1] L. Delgado,[1] and C. Cantoni[2]
[1]*Department of Mechanical Engineering and Texas Center for Superconductivity, University of Houston, 4800 Calhoun Rd., Houston, Texas 77204-4006, USA*
[2]*Oak Ridge National Laboratory, Oak Ridge, Tennessee 37381, USA*

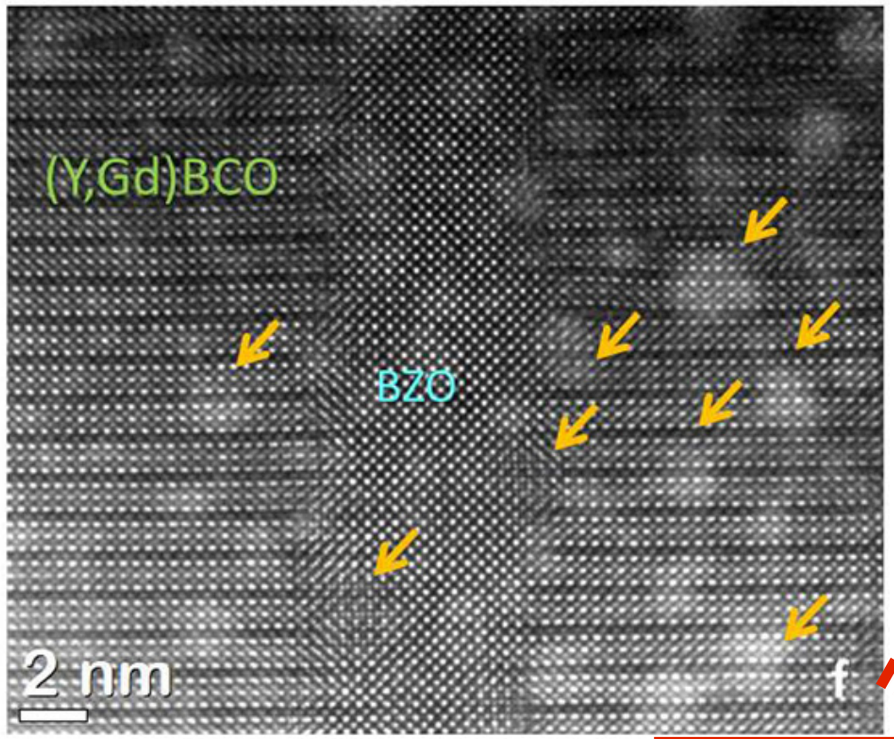

FIG. 4. Microstructures of a 25 mol. % Zr-added (Gd,Y)BCO superconductor tape made by MOCVD analyzed by cross sectional TEM (a) and (b), plan

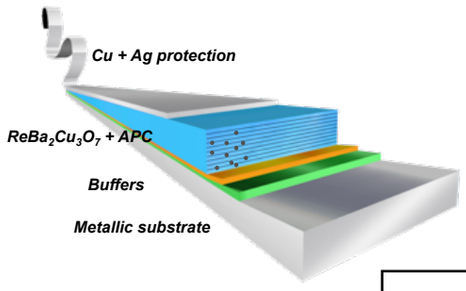

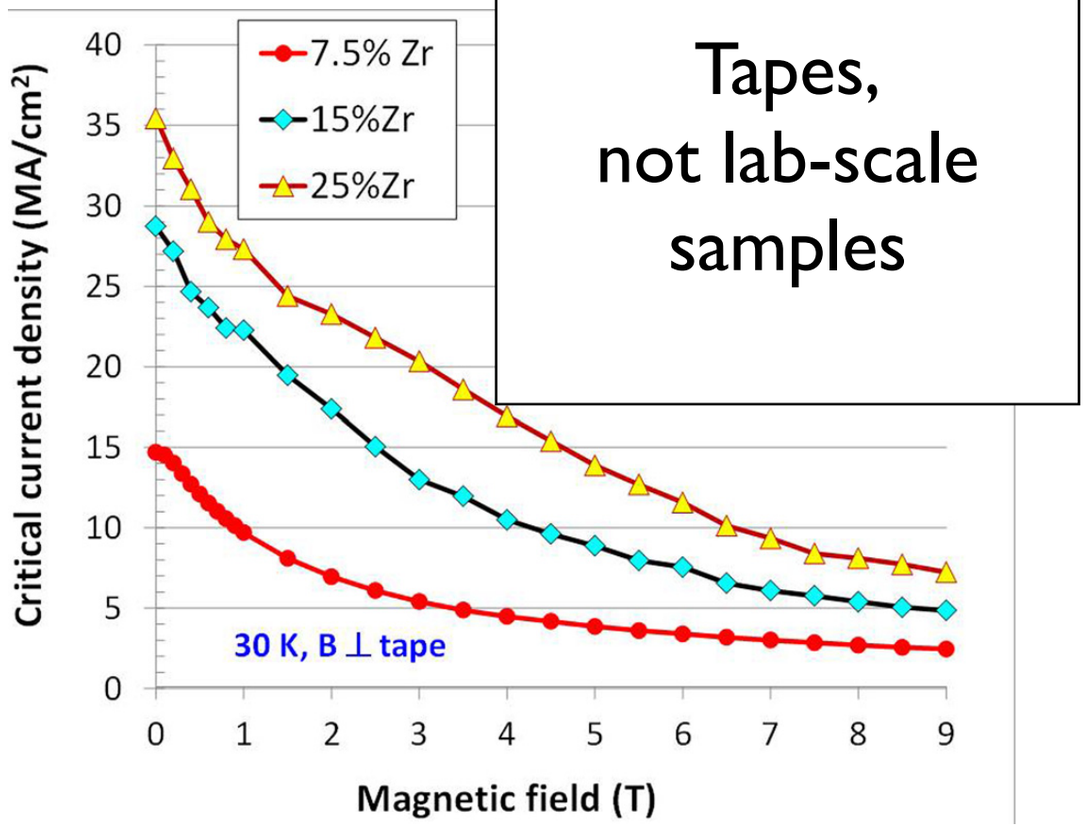

Tapes, not lab-scale samples

exceptionally robust macroscopic quantum state!

FIG. 1. Magnetic field dependence of critical current density of 7.5, 15, and 25 mol. % Zr-added (Gd,Y)BCO superconductor tapes at 30 K in the orientation of field perpendicular to tape. Inset—Pinning force characteristics of 25 mol. % Zr-added (Gd,Y)BCO superconductor tape at 30 K and 20 K in the orientation of field perpendicular to tape.

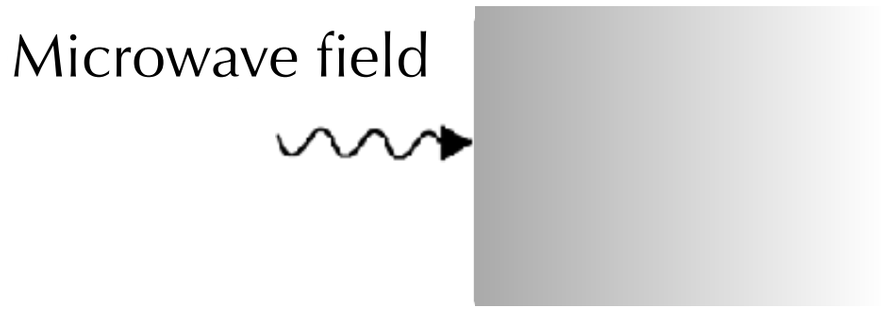

Microwave response and the mixed state

Microwave response – nomenclature

Bulk probe
(within a few λ)

Microwave field

(1–100 GHz)

At the surface:

$$\mathbf{E}_{//} = Z_s \mathbf{n} \times \mathbf{H}_{//}$$

$Z_s = R_s + iX_s$ surface impedance

$$Z_s = i\omega\mu_0\widetilde{\lambda}(H,T,\omega) = \sqrt{i\omega\mu_0\widetilde{\rho}(H,T,\omega)} = \sqrt{i\frac{\omega\mu_0}{\widetilde{\sigma}(H,T,\omega)}}$$

"screening + dissipation"
"reactance + resistance"
"out-of-phase + in-phase"

Z_s ⇔ $\widetilde{\lambda}$ ⇔ $\widetilde{\sigma}$ ⇔ $\widetilde{\rho}$

surface impedance ⇔ effective penetration depth ⇔ complex conductivity ⇔ complex resistivity

The classical ("cavity people") view

- Two fluid model (or BCS)

$$\sigma_1 = \frac{n_n e^2 \tau}{m}$$

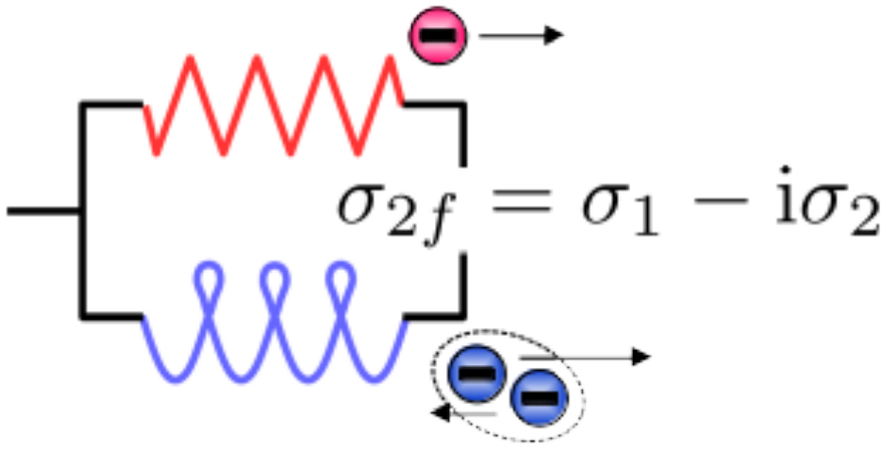

$$\sigma_2 = \frac{n_s e^2}{m\omega} = \frac{\omega \mu_0}{\lambda^2}$$

$$\tilde{\rho} = \frac{1}{\sigma}$$

$$Z_S = \sqrt{\frac{i\omega\mu_0}{\sigma}} + R_{res}$$

"The cleaner the material, the better"

(low R_{res})

but…

Microwave response – nomenclature

Bulk probe
(within a few λ)

Microwave field

(1–100 GHz)

At the surface:

$$\mathbf{E}_{//} = Z_s \mathbf{n} \times \mathbf{H}_{//}$$

$Z_s = R_s + iX_s$ surface impedance

$$Z_s = i\omega\mu_0\widetilde{\lambda}(H,T,\omega) = \sqrt{i\omega\mu_0\widetilde{\rho}(H,T,\omega)}$$

vortex motion in the complex resistivity !

$$\widetilde{\rho} = \frac{\rho_{vm} + i\frac{1}{\sigma_2}}{1 + i\frac{\sigma_1}{\sigma_2}}$$

Superfluid/quasiparticle contribution to R_s is irrelevant with respect to vortex motion!

Microwave response – Thin films

Microwave field

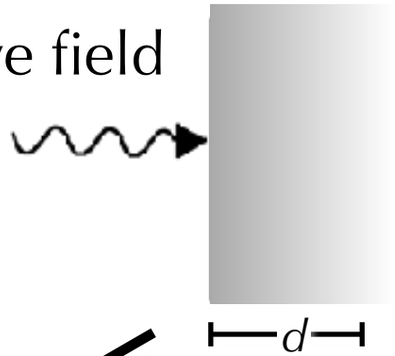

Bulk probe
(within a few λ)

At the surface:

$$\mathbf{E}_{//} = Z_s \mathbf{n} \times \mathbf{H}_{//}$$

$Z_s = R_s + iX_s$ surface impedance

bulk

$$Z_s = \sqrt{i\omega\mu_0\widetilde{\rho}(H,T,\omega)}$$

thin film $d < \lambda$

$$Z_s \approx \frac{\widetilde{\rho}(H,T,\omega)}{d}$$

Thin film: complexities due to different substrates.
Care in the extraction of superconducting parameters:

Metallic (coated conductors)

N. Pompeo et al., IEEE TAS 28, 9000505 (2018)
J. Phys.: Conf. Ser. 1065 052018 (2018)

Para/ferroelectric ($SrTiO_3$)

N. Pompeo et al., SuST 20, 1002 (2007)
N. Pompeo et al. Proc. IEEE I2MTC 2017 doi: 10.1109/I2MTC.2017.7969902

Semiconductors

N. Pompeo, R. Marcon, L. Méchin, E. Silva, SuST 18, 531 (2005)

Microwave response – $H_{dc} \neq 0$: vortex motion

Bulk probe
(within a few λ)

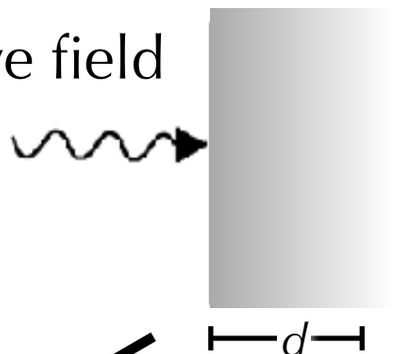

At the surface:

$$\mathbf{E}_{//} = Z_s \mathbf{n} \times \mathbf{H}_{//}$$

$Z_s = R_s + iX_s$ surface impedance

bulk

$$Z_s = \sqrt{i\omega\mu_0 \widetilde{\rho}(H,T,\omega)}$$

thin film $\quad d < \lambda$

$$Z_s \approx \frac{\widetilde{\rho}(H,T,\omega)}{d}$$

Driven vortices → complex resistivity

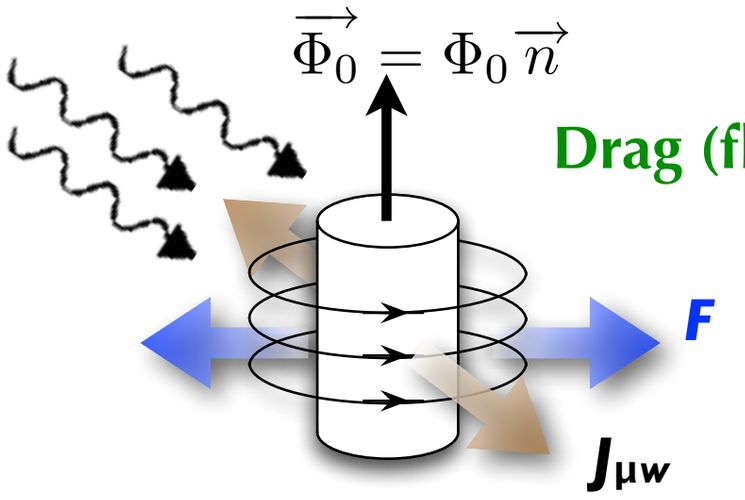

Drag (flux flow)

+

elastic recall (pinning)

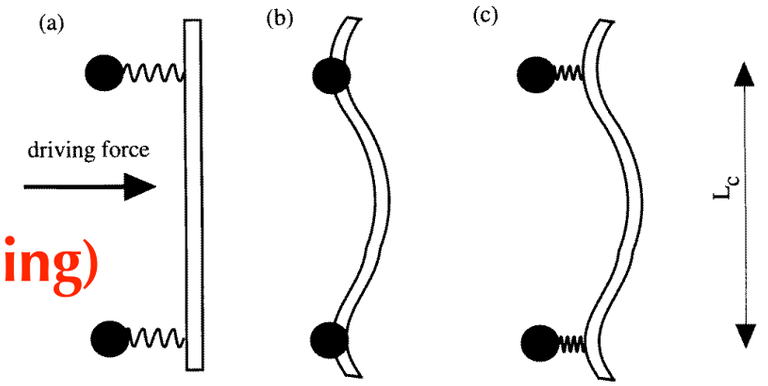

Fig. by M. Golosovsky et al, SuST. 9 (1996) 1–15.

Vortex motion at microwaves

Microwaves:

vortex shaking

- **subcritical current: <u>linear regime</u>**
- negligible perturbation on pinning potential
- very small rms vortex displacements (≪ 1nm)

⇒ vortex-vortex interaction relevant
for the **static** arrangement only

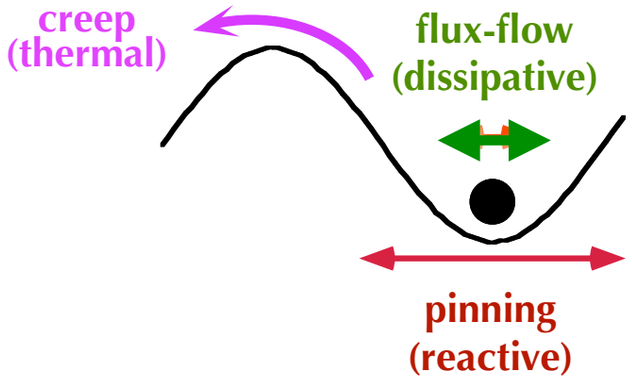

- dissipation+reactance (two observables)

DC (J_c, ρ_{dc}):

vortex drag

- large current: **<u>strongly nonlinear regime</u>**
- strongly tilted washboard potential
- large vortex displacement

⇒ vortex-vortex interaction relevant
in the **dynamics**
(vortex fluids, molasses, etc etc)

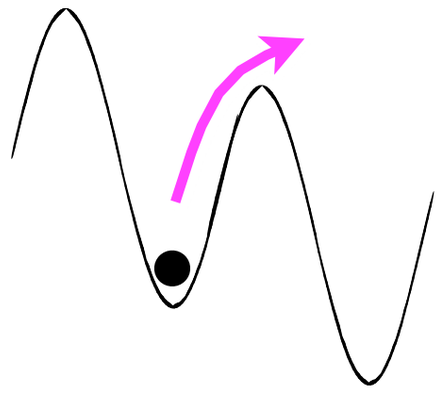

- technical issues
(heating, large currents, ...)

Vortex motion at microwaves

Microwaves:

vortex shaking

- **subcritical current: linear regime**
- negligible perturbation on pinning potential
- very small rms vortex displacements (≪ 1nm)

⇒ vortex-vortex interaction relevant for the **static** arrangement only

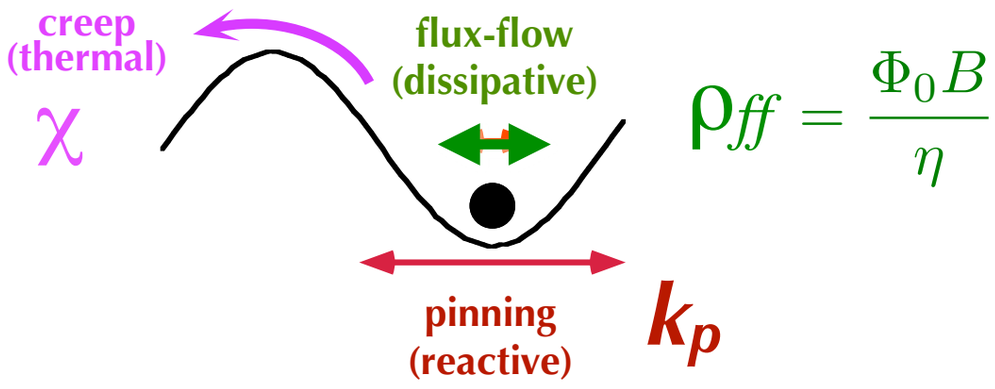

$$\eta\mathbf{v} + k_p\mathbf{x} = \mathbf{J} \times \hat{\mathbf{n}}\Phi_0 + \mathbf{F_{thermal}}$$

* Gittleman, Rosenblum PRL 16 734 (1966) — *No creep*
Coffey, Clem PRL 67 386 (1991) — *Sinusoidal potential*
Brandt PRL 67 2219 (1991) — *Thermally relaxing kp*
Placais, Mathieu, Simon, Sonin, Traito, PRB 54 13083 (1996) — *Two-mode*

** *N. Pompeo, E.Silva PRB 78, 094503 (2008)*

vortex motion complex resistivity

Many models*,one equation**:

$$\rho_{v1}(H) + \mathrm{i}\rho_{v2}(H) = \rho_{ff}\frac{\chi + \mathrm{i}\frac{\nu}{\nu_0}}{1 + \mathrm{i}\frac{\nu}{\nu_0}}$$

1. **depinning frequency**

$\nu_0 \rightarrow \nu_p = k_p/2\pi\eta$

($\nu_p \neq \nu_0$: "depinning frequency")

pinning constant

(elastic recall)

$$k_p = \nu_p\eta$$

2. **flux-flow resistivity**

$$\rho_{ff} = \Phi_0 B/\eta$$

3. ***creep factor*** χ

vs. *T*, *H*, θ

High frequency vortex motion

Even strongly pinned vortices oscillates

- dissipation arises
- elastic recall from pinning centers
- flux creep

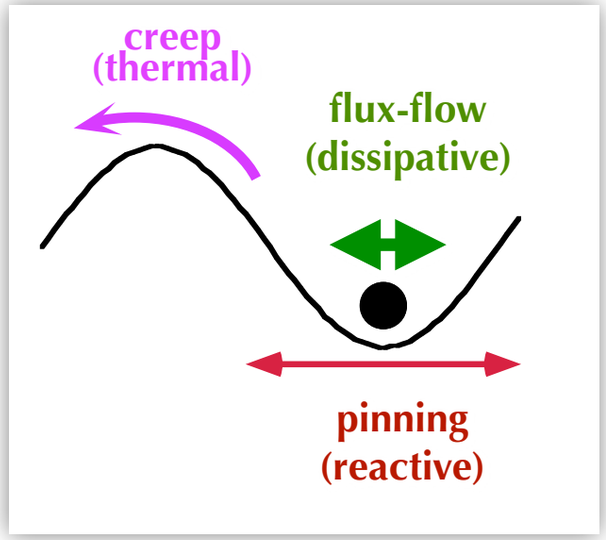

$$\Delta\rho_1(H) + \mathrm{i}\Delta\rho_2(H) = \rho_{ff}\frac{\chi + \mathrm{i}\frac{\nu}{\nu_0}}{1 + \mathrm{i}\frac{\nu}{\nu_0}}$$

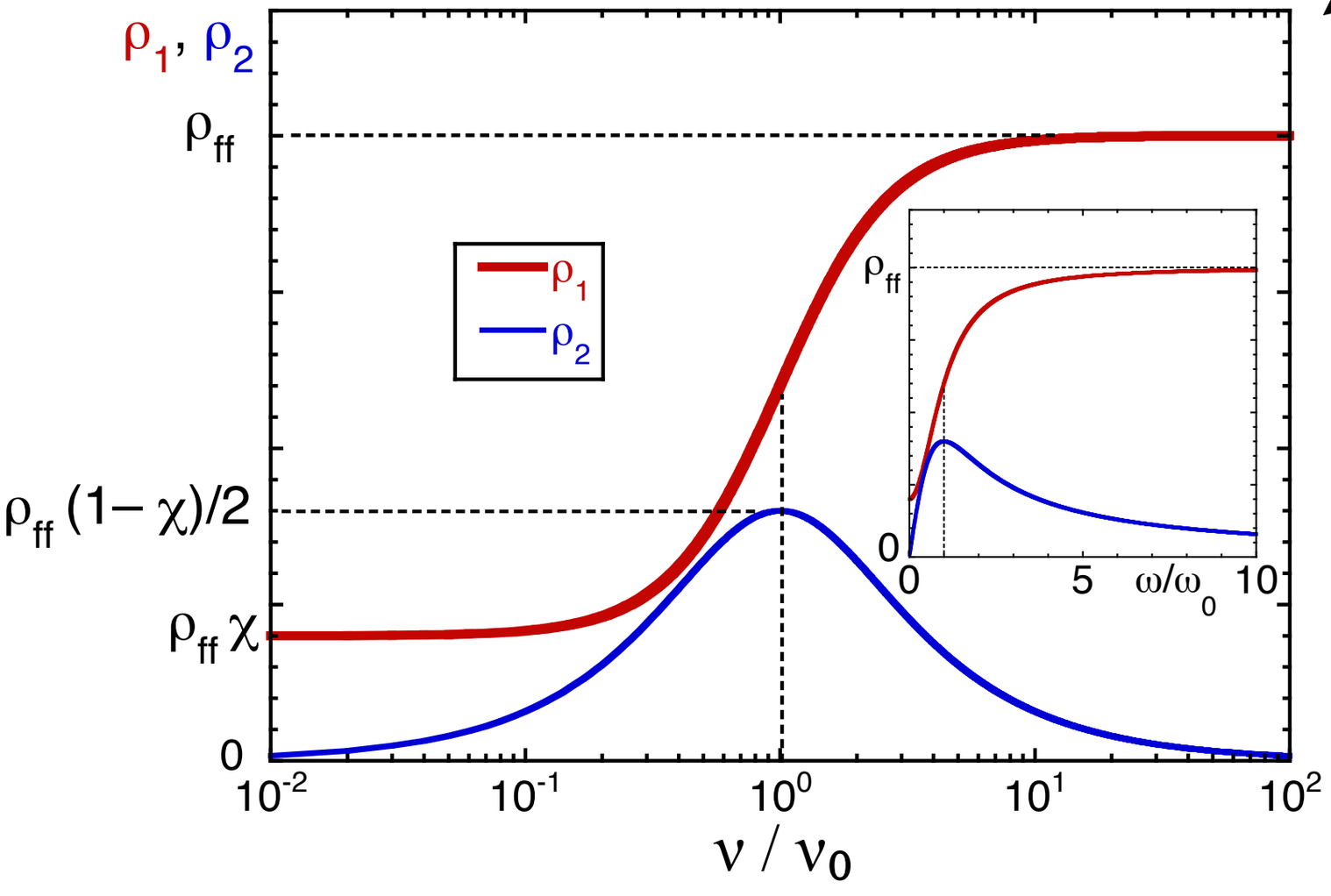

1. **depinning frequency**

$$\nu_0 \rightarrow \nu_p = k_p/2\pi\eta$$

($\nu_p \neq \nu_0$: "depinning frequency")

pinning constant
(elastic recall)

$$k_p = \nu_p\eta$$

2. **flux-flow resistivity**

$$\rho_{ff} = \Phi_0 B/\eta$$

3. ***creep factor*** χ

vs. *T*, *H*, θ

High frequency vortex motion

Decrease losses at fixed ν: high ν_0, small losses:

- high k_p: strong pinning. Can be engineered (to a point)
- small ρ_{ff}. Cannot be engineered, microscopic state

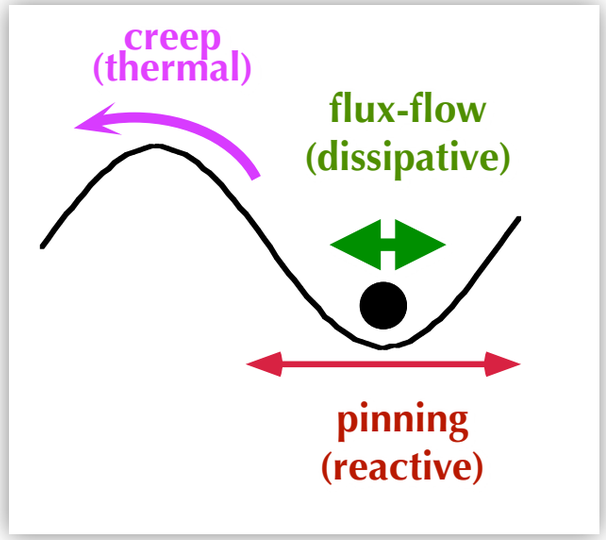

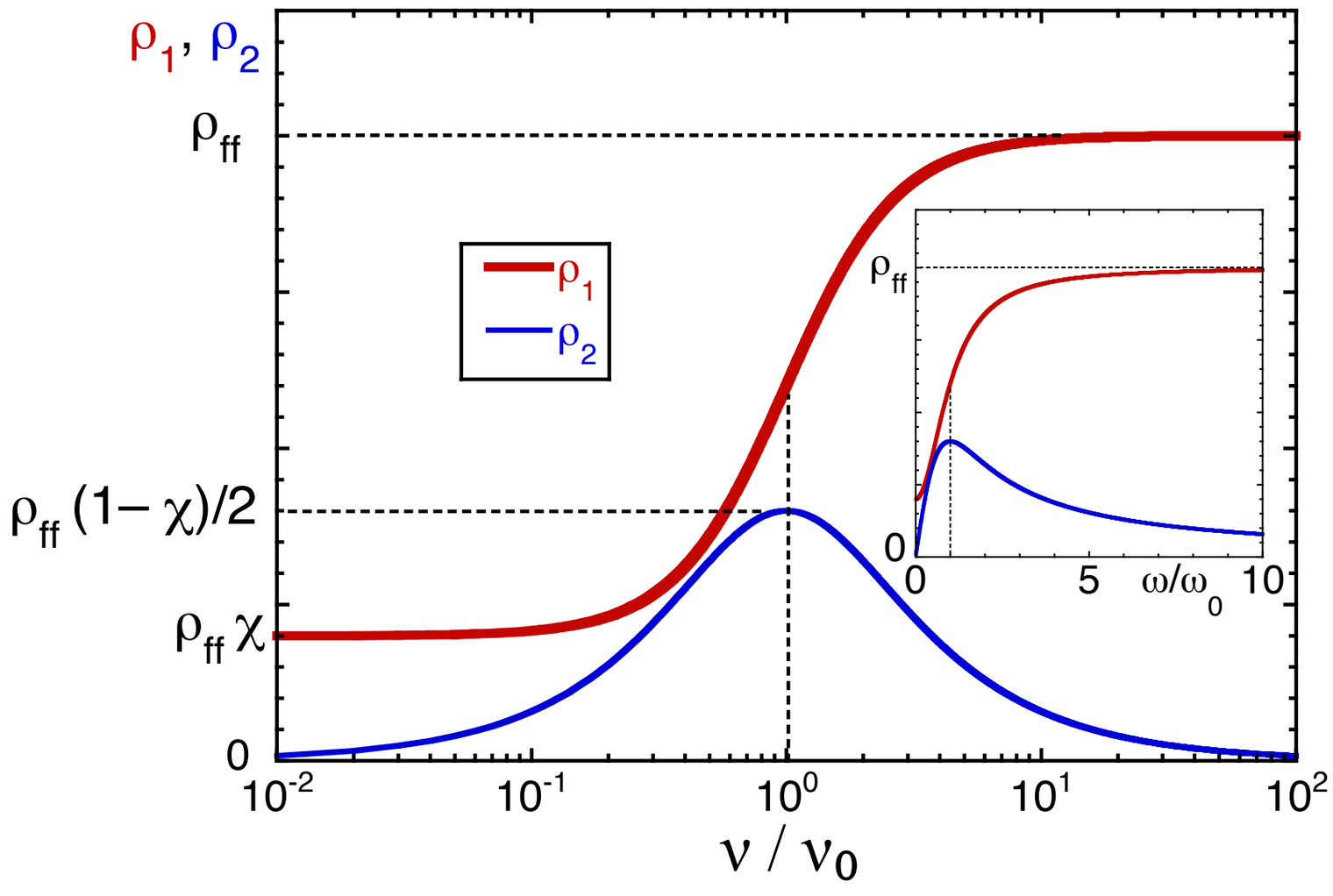

1. **depinning frequency**

$$\nu_0 \rightarrow \nu_p = k_p/2\pi\eta$$

($\nu_p \neq \nu_0$: "depinning frequency")

pinning constant
(elastic recall)

$$k_p = \nu_p \eta$$

2. **flux-flow resistivity**

$$\rho_{ff} = \Phi_0 B/\eta$$

3. ***creep factor*** χ

vs. *T*, *H*, θ

High frequency vortex motion complex resistivity

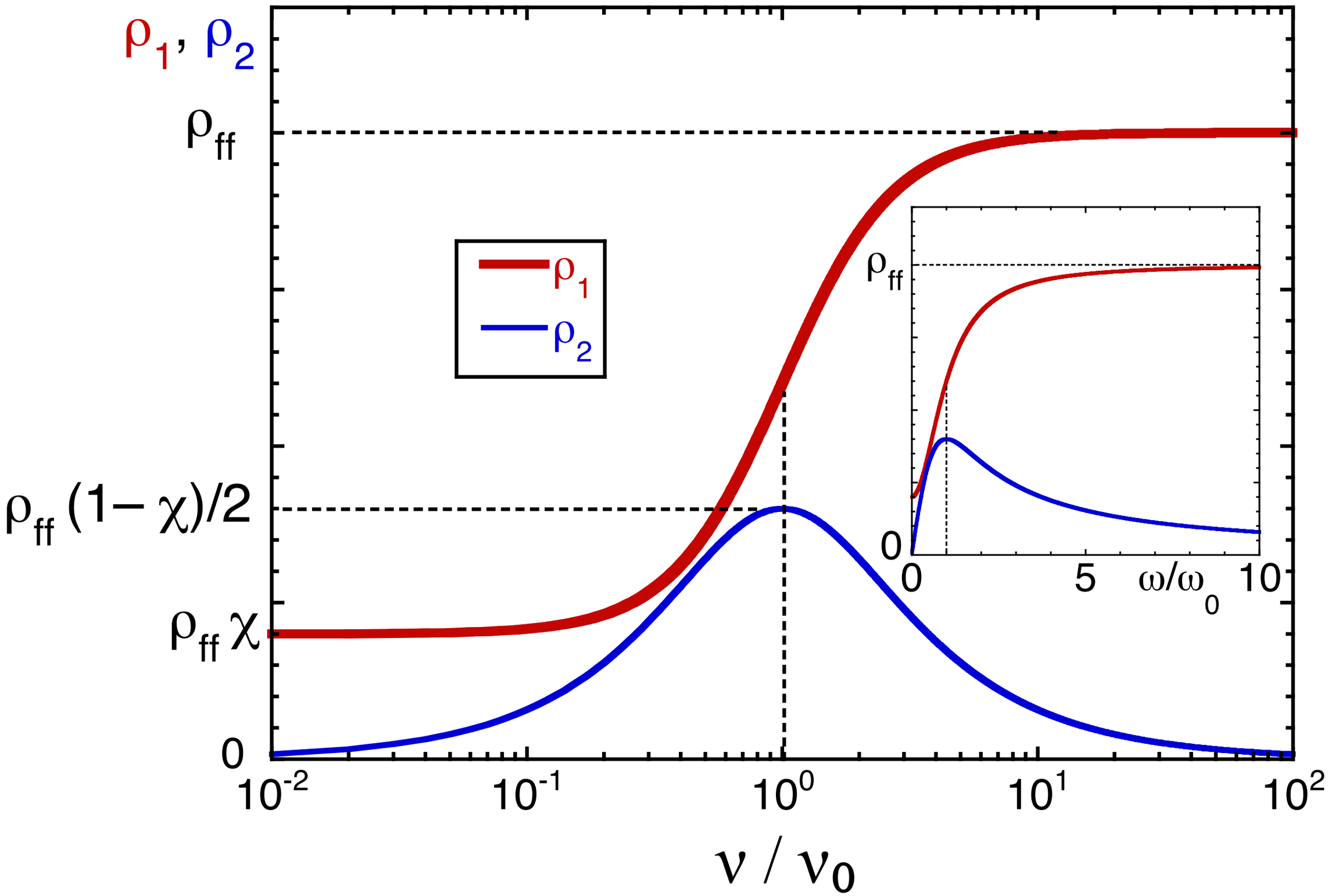

Surface impedance

$$\Delta Z_S = Z_S(H) - Z_S(0)$$

$k_p = 4 \times 10^4$ Nm^{-2}
$\eta = 3 \times 10^{-7}$ Nsm^{-2}
(appropriate for $YBa_2Cu_3O_7$ thin films around 60 K)
$\rightarrow \omega_p = 2\pi \cdot 21$ GHz.
Small symbols:
same parameters, with $\chi = 0.1$

BCS R_s irrelevant!

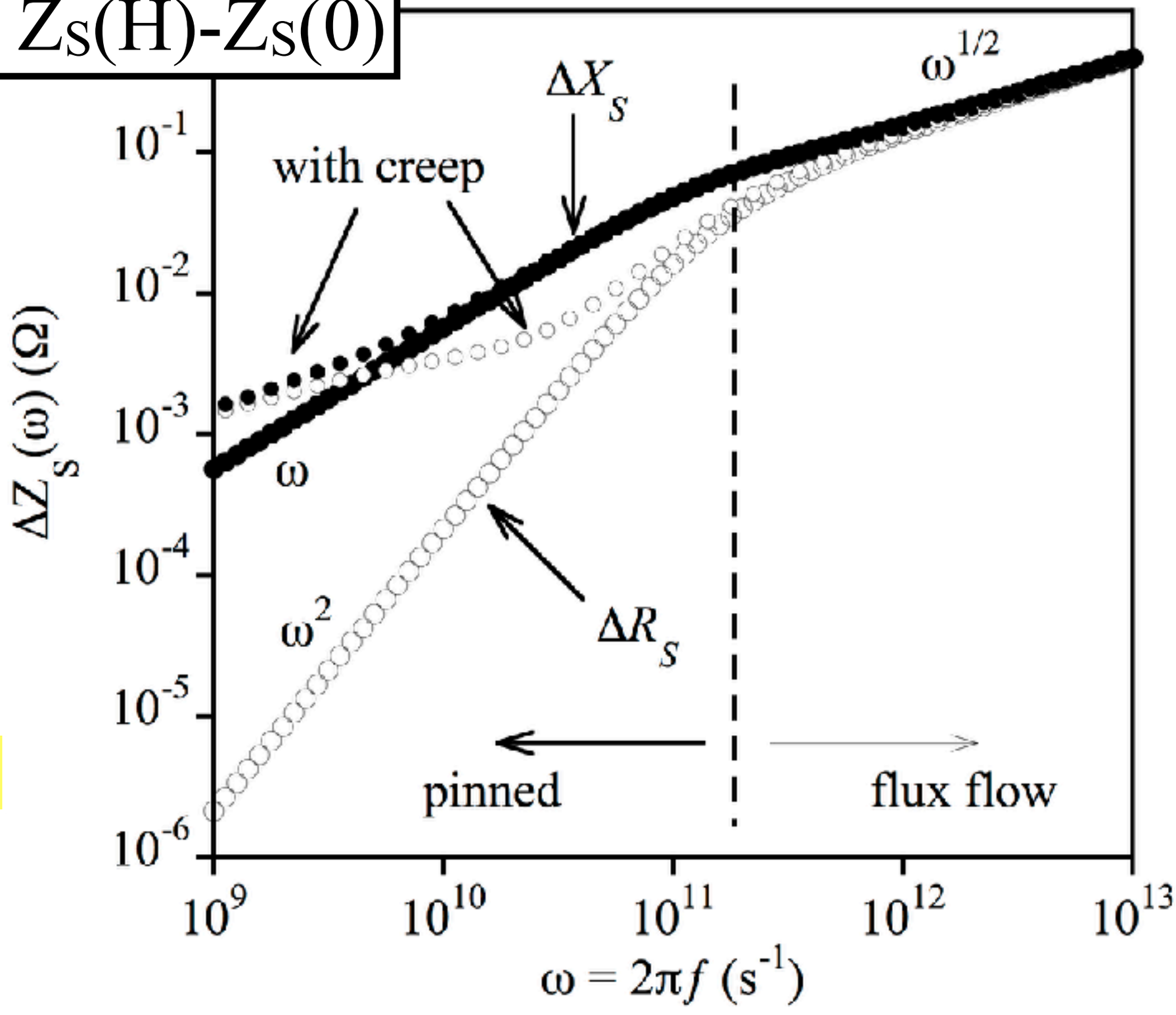

Why?

Motivation: physics - flux flow

ρ_{ff}, η

Flux-flow: **free** motion of vortices (pinning irrelevant)

ρ_{ff} → Physics of the vortex core: fundamental processes

A window on quasiparticles in the mixed state

"Bardeen-Stephen $\rho_{ff} = \rho_n \frac{B}{B_{c2}(T)}$

(+ maybe corrections)"

$$\rho_{ff} = \rho_n \frac{1}{\beta(T)} \frac{B}{B_{c2}(T)}$$

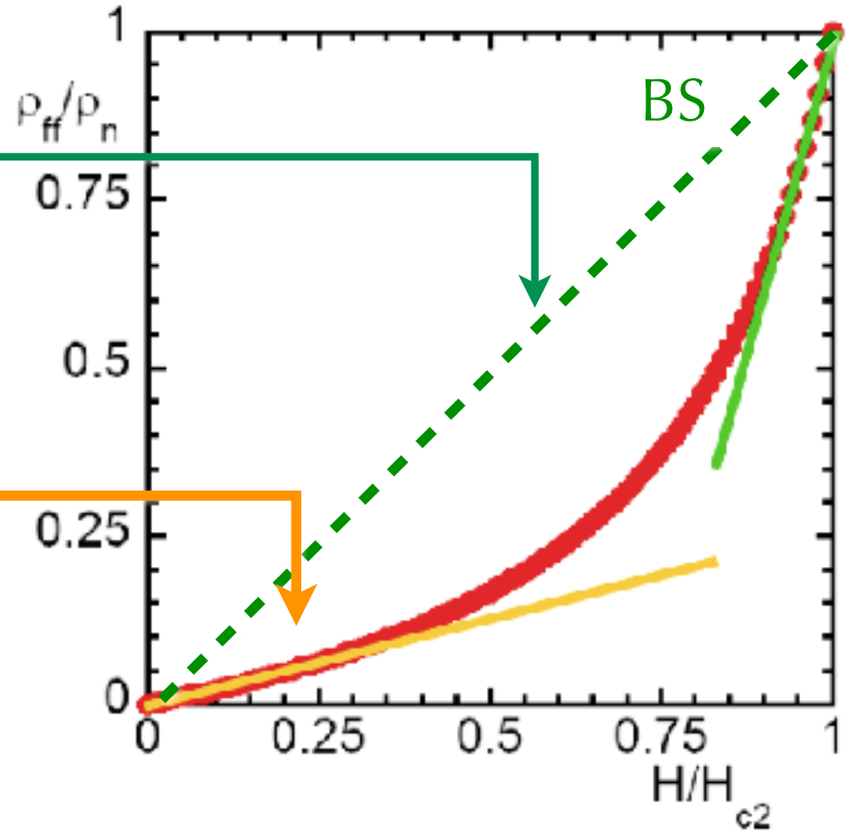

Motivation: physics - pinning

k_p Material science: pinning constant measures the ***steepness*** of the pinning well

$$F = -k_p x$$

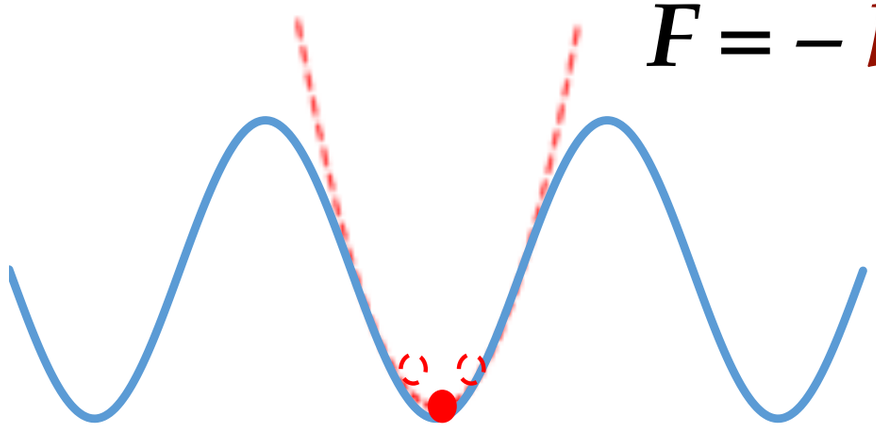

⇒ optimization of the pinning landscape

(complementary information to J_c → *heigth* of the pinning well)

ν_p Depinning frequency: crossover between low and high losses regimes (→ applications in H≠0)

Motivation: physics - anisotropy

ρ_{ff}, k_p, γ

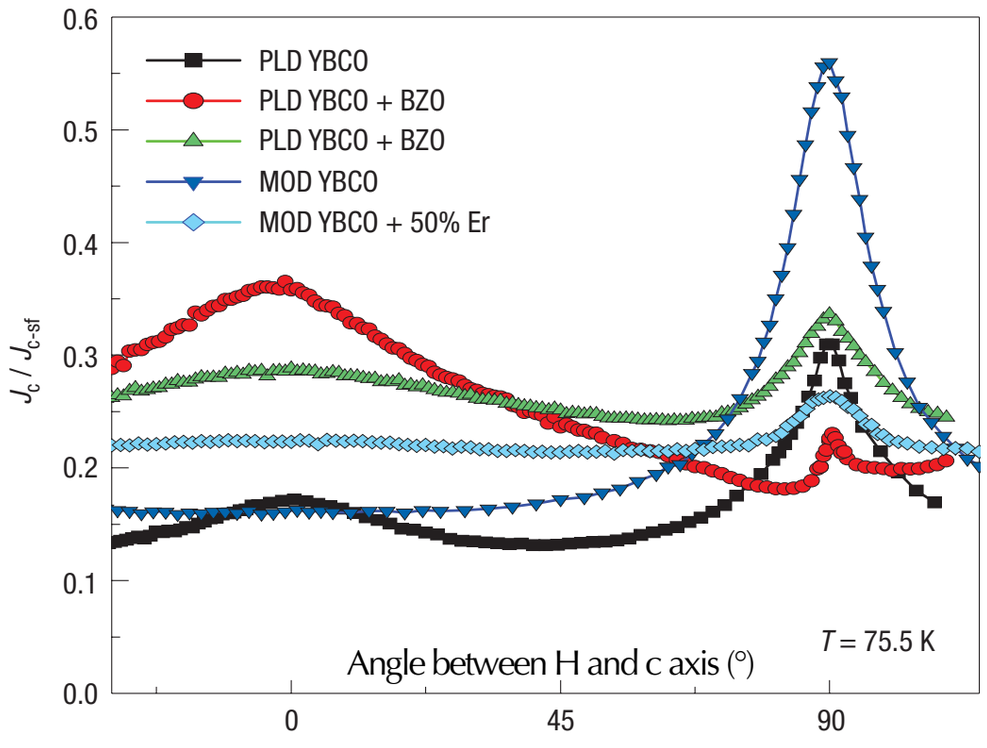

Directional pinning:
dramatic effect on J_c anisotropy.

Do defects change the microscopic state
(i.e. the mass anisotropy)?

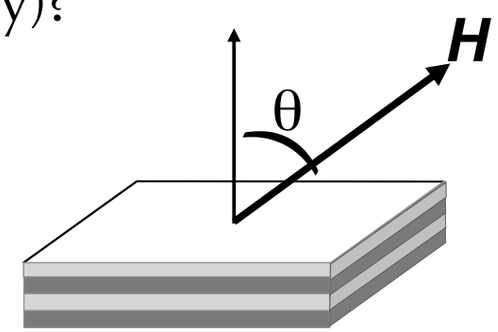

S. R. Foltyn, l. Civale,
J. l. MacManus-Driscoll, Q. X. Jia,
B. Maiorov, H. Wang and M. Maley
Nature Materials vol.6, 631 (2007)

Measured anisotropy:

mass anisotropy + extended defects

"intrinsic" → $\gamma = \frac{H_{c2||}}{H_{c2\perp}}$

"effective" → γ_{eff}

Microwave measurements disentangle

ρ_{ff} does **not** depend on pinning

k_p strongly depends on pinning

Motivation: FCC beam screen

ν_p

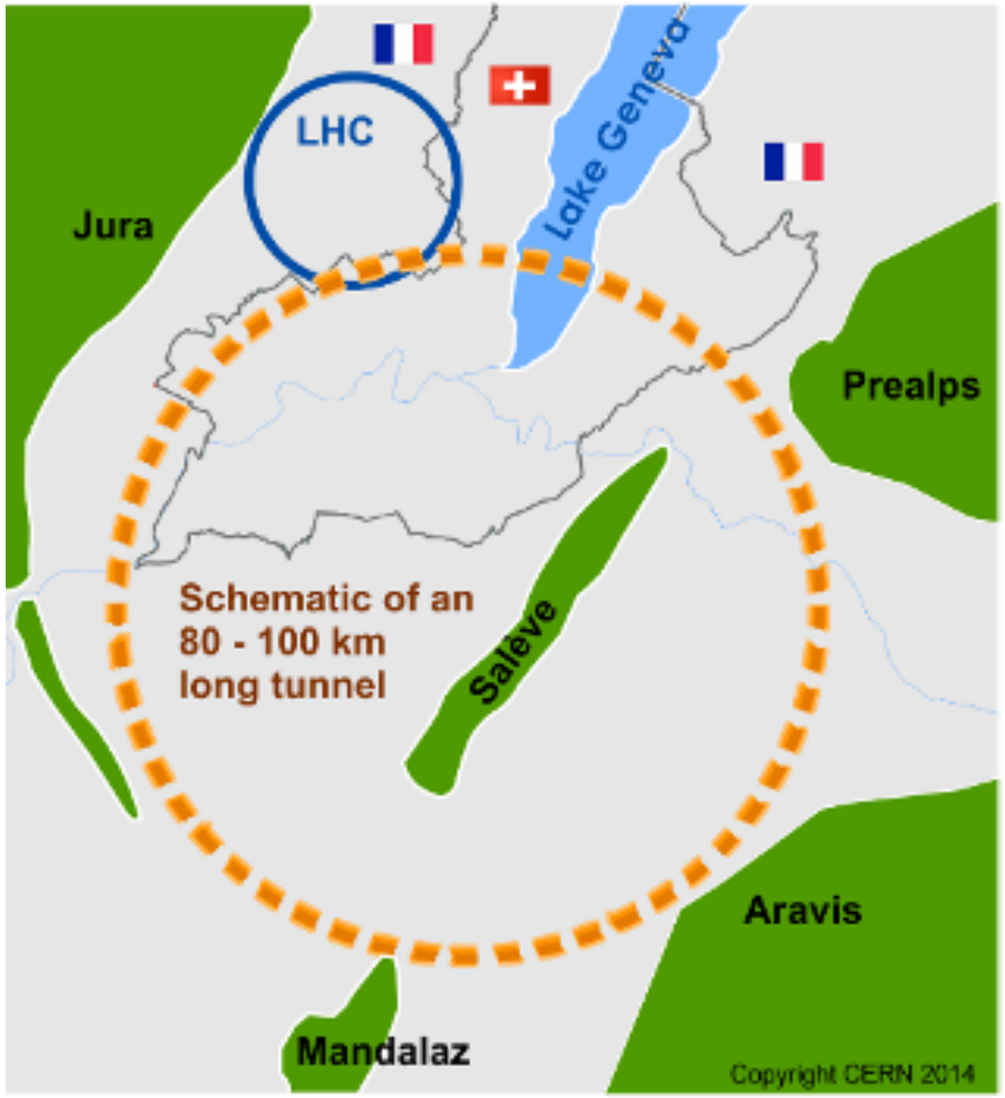

Low R_s for wake fields from travelling charged particles. "Beam-screen"

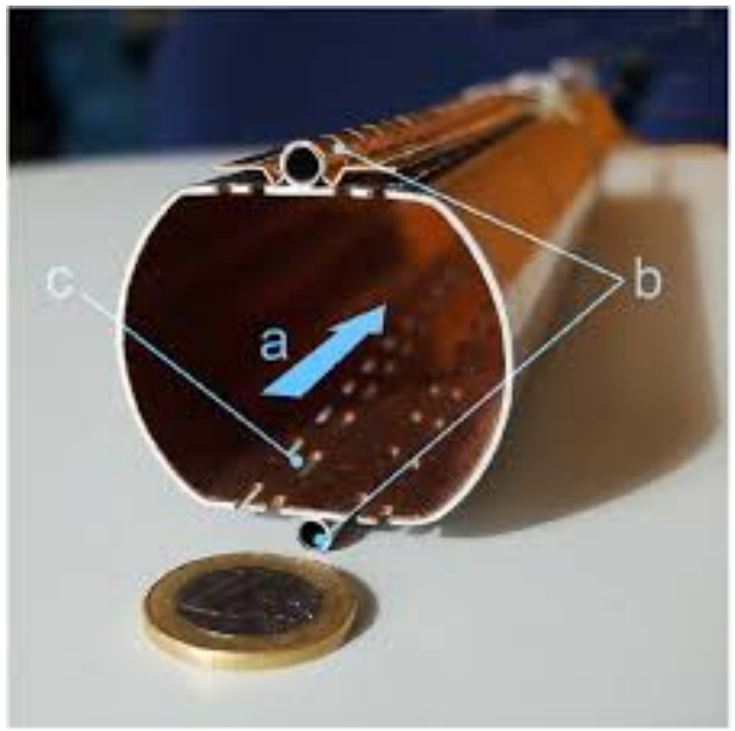

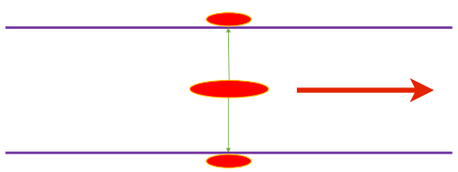

Operates in high-field: 16 T!
(care to energy content at low frequency, below 2 GHz)

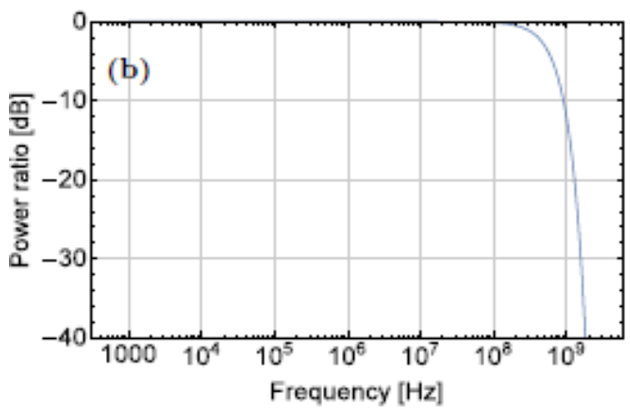

→ high depinning frequency ν_p

Motivation: Axion detectors

ν_p

- Cavity experiments for axion detections

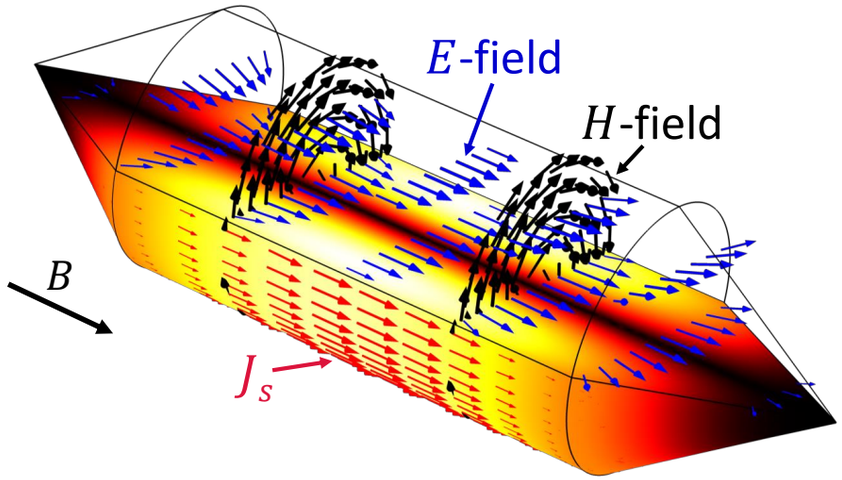

Figure 1. Electromagnetic simulation of the haloscope excited with the TM_{010} mode. The distributions of the radio frequency electric E-field (in blue), the magnetic H-field (in black), and the surface current density J_s (in red) are shown. The direction of the externally applied static B field is shown to be parallel to the longitudinal axis of the cavity.

Operates in "moderate" fields: few T
Operating frequency 5-25 GHz
High Q required (above Cu)
⇒ low R_s

J.S. Sloan et al,
Physics of the dark universe
14, 95-102 (2016)

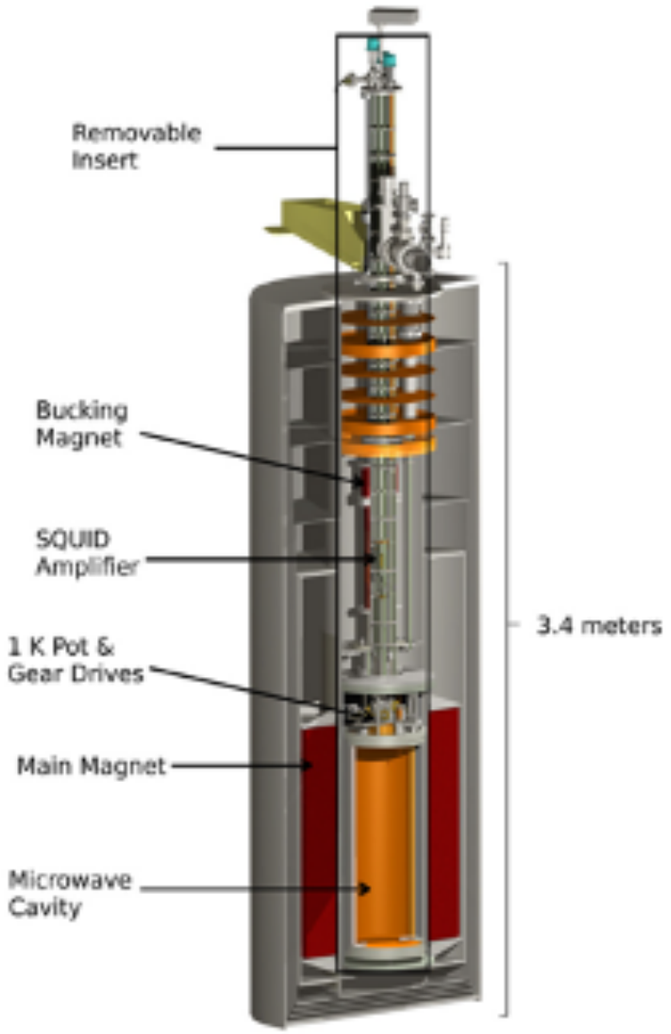

→ high depinning frequency ν_p

Experimental method:
the dielectric resonator

Measurements: resonators technique

Here of interest:
surface perturbation

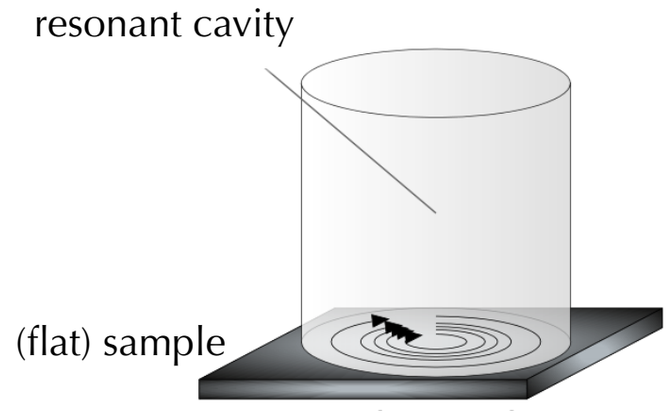

Measurand vs. ν at various T e H: scattering coefficients

S_{ij}

line calibration

Quality factor, resonant frequency

$Q \quad \nu_0$

Maxwell

variation of the surface resistance and reactance

$\Delta R_S \quad \Delta X_S$

Thin film (⚠)

variation of the complex resistivity

$\Delta\rho_1 \quad \Delta\rho_2$

Calibration of the resonator

$R_S \quad \Delta X_S$

Additional assumptions, reference measurements

$R_S \quad X_S$

Difficulties:
- calibrations
- cryogenics (down to 3 K)
- high magnetic fields (up to 12 T)

Dielectric loaded resonators

$$\frac{1}{Q} = \frac{R_s}{G_s} + \frac{R_m}{G_m} + \eta \tan \delta_\epsilon$$

$$-2\frac{\Delta\nu_0}{\nu_0} = \frac{\Delta X_s}{G_s} + \frac{\Delta X_m}{G_m} + \eta \frac{\Delta \epsilon'_r}{\epsilon'_r}$$

variation of X_S (e.g., with *T* or *H*)

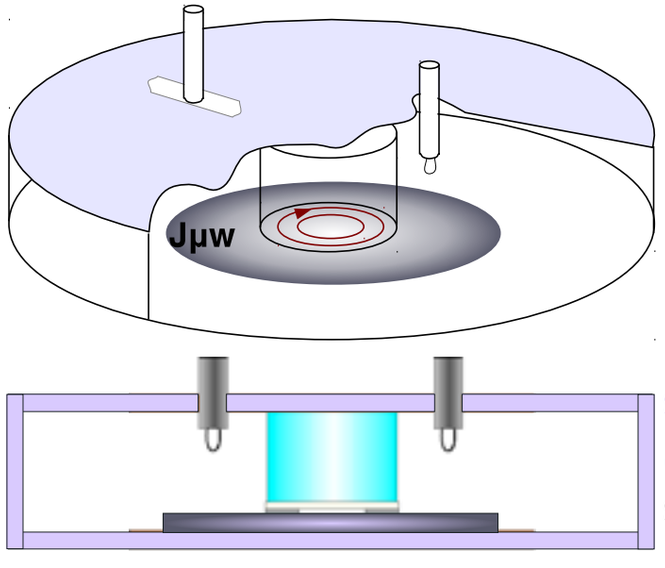

16, 27 GHz dual mode sapphire resonator.

8 GHz rutile resonator.

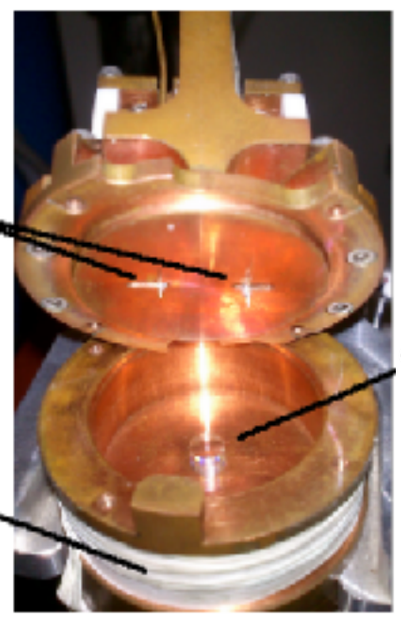

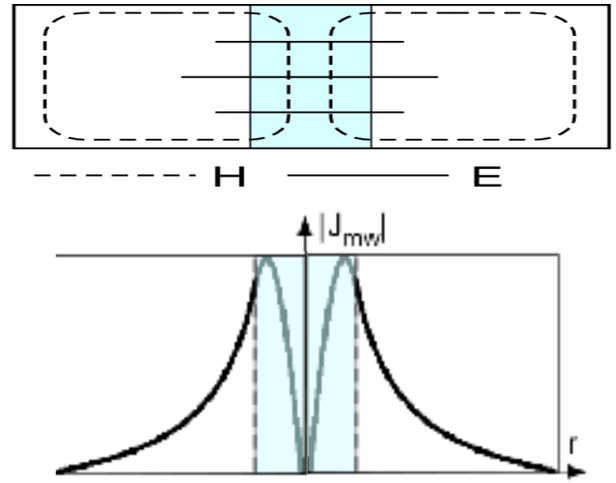

"Hakki-Coleman".
TE_{011}: high *Q*, planar and circular currents

N. Pompeo et al., Meas. Sci. Rev. 14, 164 (2016)
K. Torokhtii et al J. Phys.: Conf. Ser. 1065 052027 (2018)
A. Alimenti et al., Meas. Sci. Technol., 30, 065601 (2019)

Dielectric loaded resonators

$$\frac{1}{Q} = \frac{R_s}{G_s} + \frac{R_m}{G_m} + \eta \tan\delta_\epsilon$$

$$-2\frac{\Delta\nu_0}{\nu_0} = \frac{\Delta X_s}{G_s} + \frac{\Delta X_m}{G_m} + \eta\frac{\Delta\epsilon_r'}{\epsilon_r'}$$

variation of X_S (e.g., with *T* or *H*)

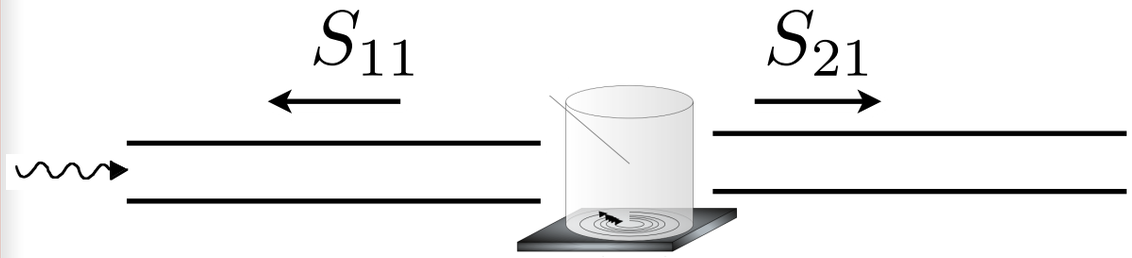

16, 27 GHz dual mode sapphire resonator.

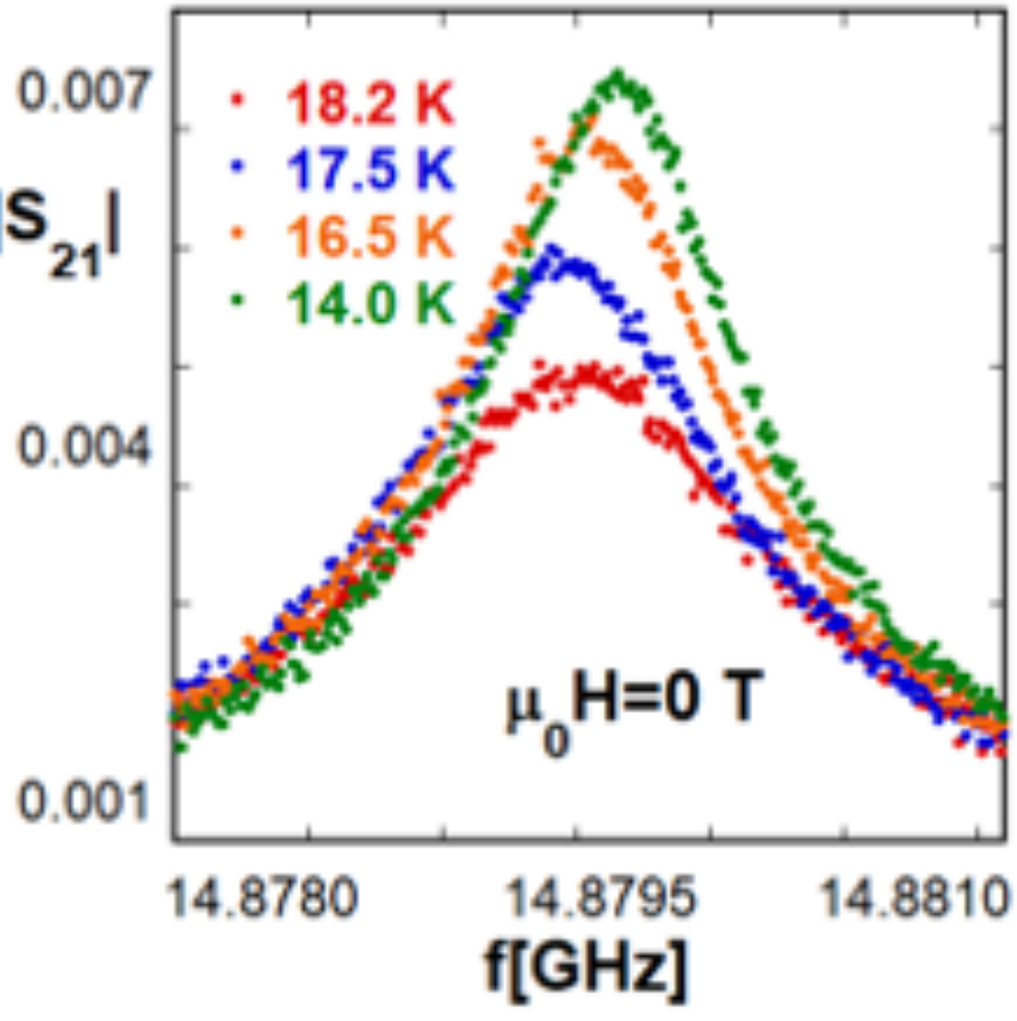

Nb_3Sn

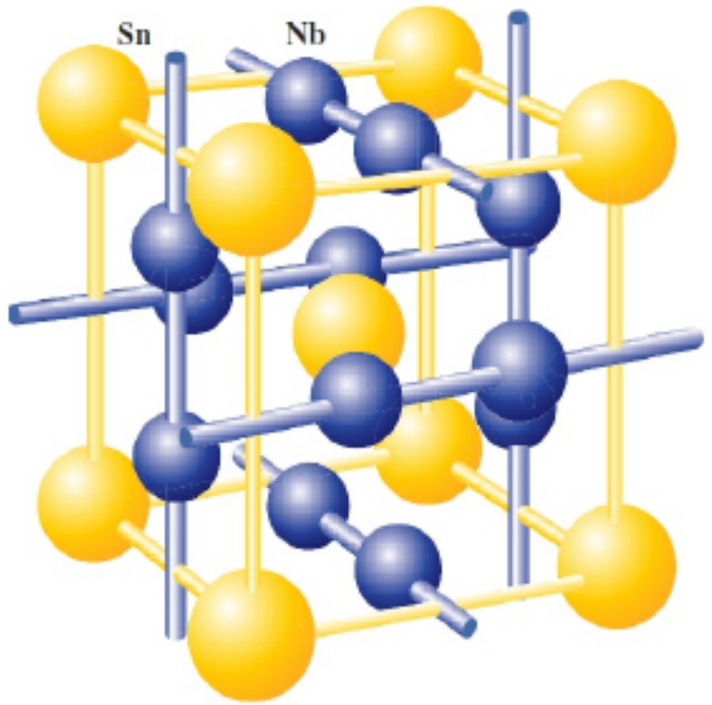

Flux-flow:
a Bardeen-Stephen case

Depinning frequency: promising for specific applications

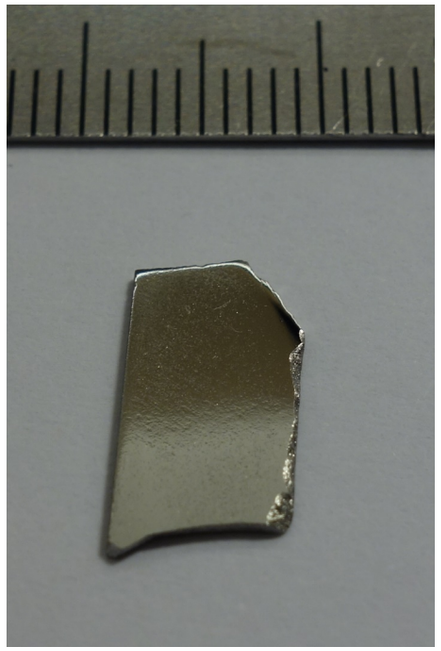

Samples:
R. Flükiger, T. Spina

bulk polycrystalline Nb_3Sn platelets
sintering Nb & Sn powder mixture in Ar under Hot Isostatic Pressure

Grain size 20 µm

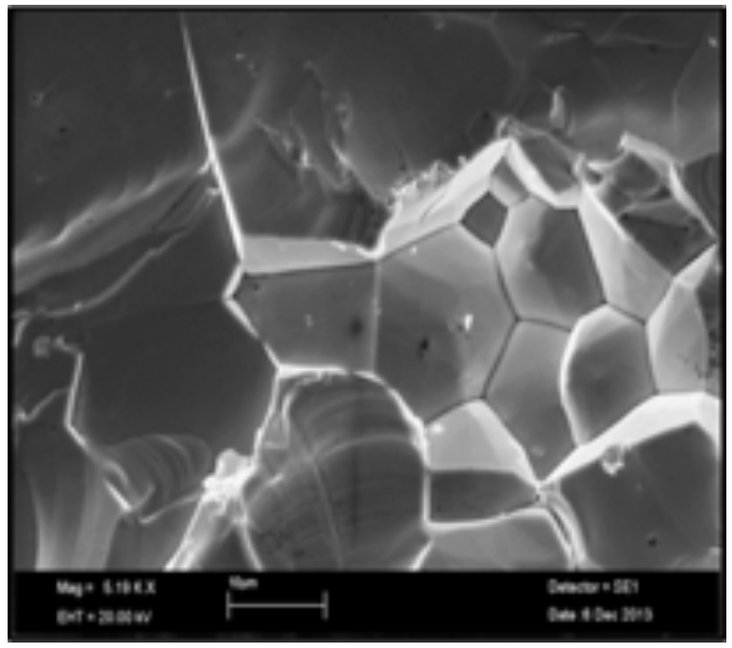

Nb_3Sn: surface impedance, 15 GHz

Field-cooled transitions

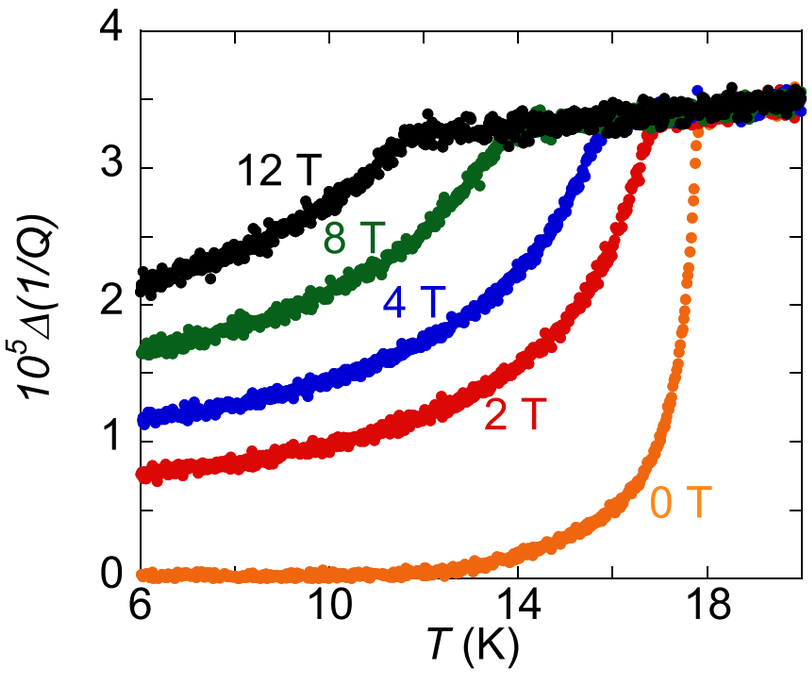

(a)

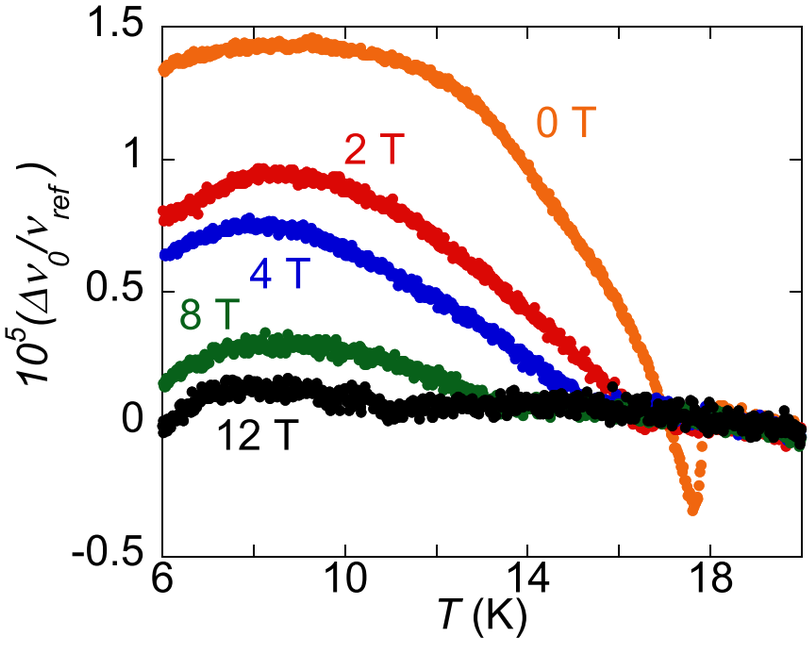

(b)

ZFC field sweeps

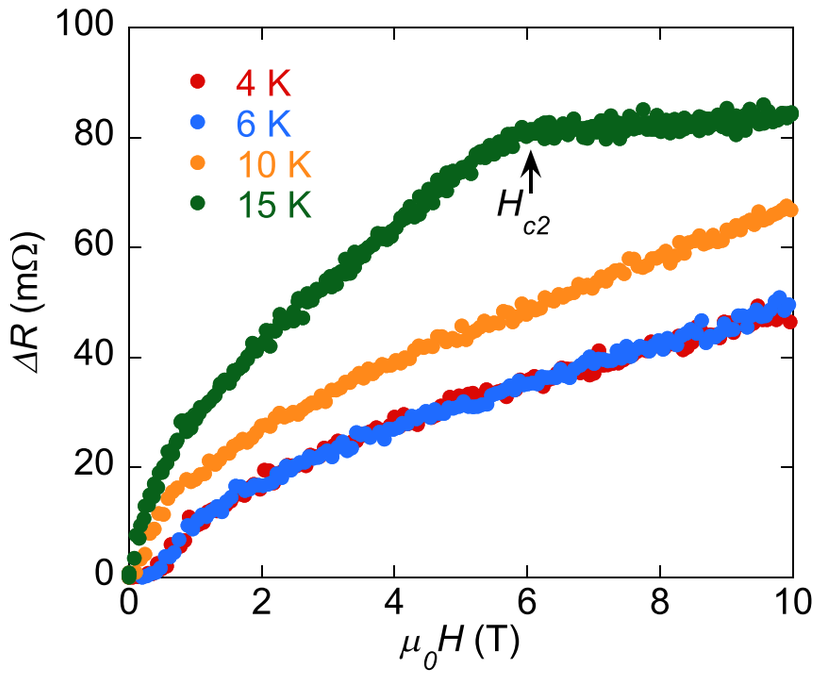

(a)

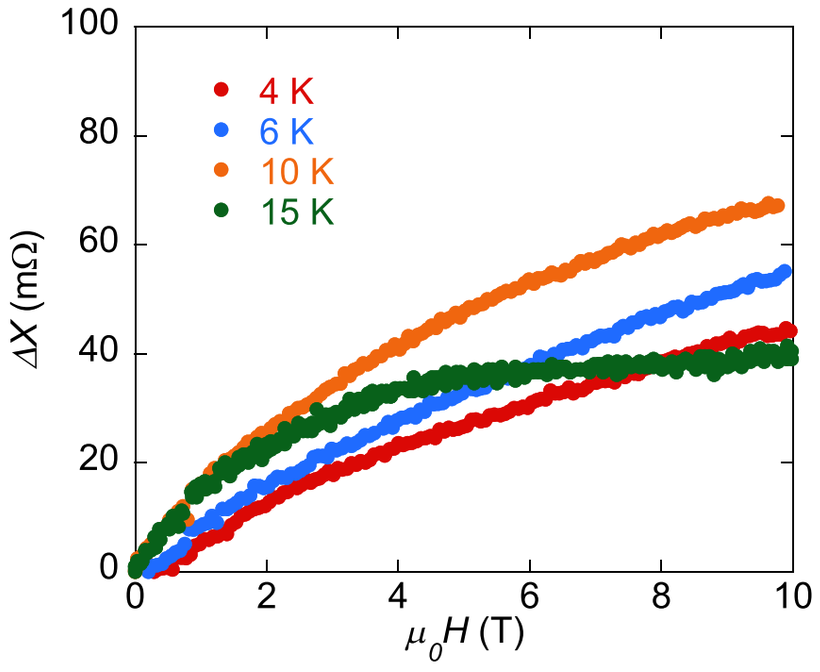

(b)

A. Alimenti et al., Supercond. Sci. Technol. 34 (2021) 014003
IEEE Trans. Appl. Supercond. 29 (2019) 3500104

Nb_3Sn: flux flow resistivity

$$Z_S = R_s + iX_s \Rightarrow \rho_1 + i\rho_2 \Rightarrow \quad \rho_{ff}$$

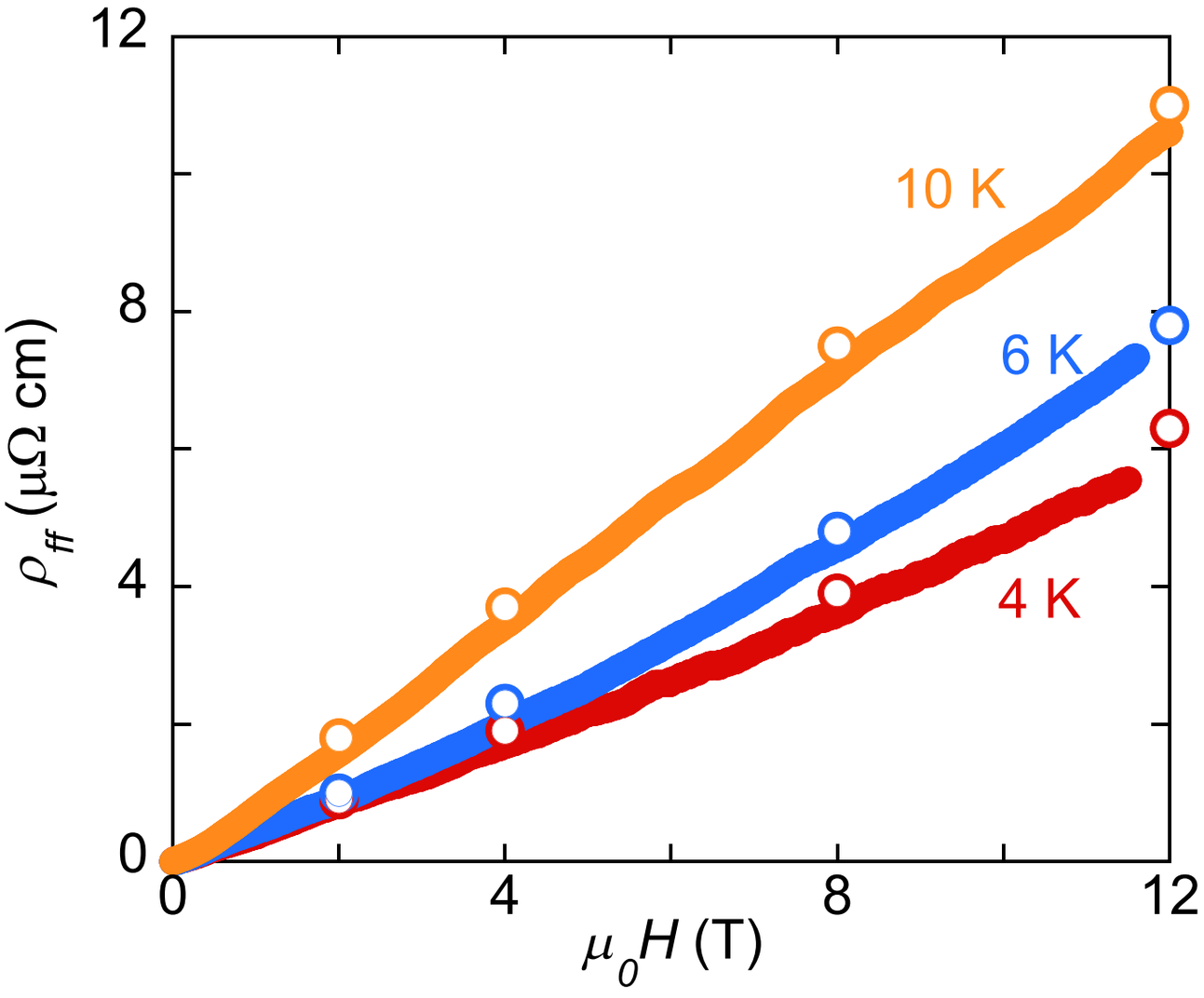

conventional
Bardeen-Stephen

$$\rho_{ff} = \rho_n \frac{H}{H_{c2}}$$

Upper critical field

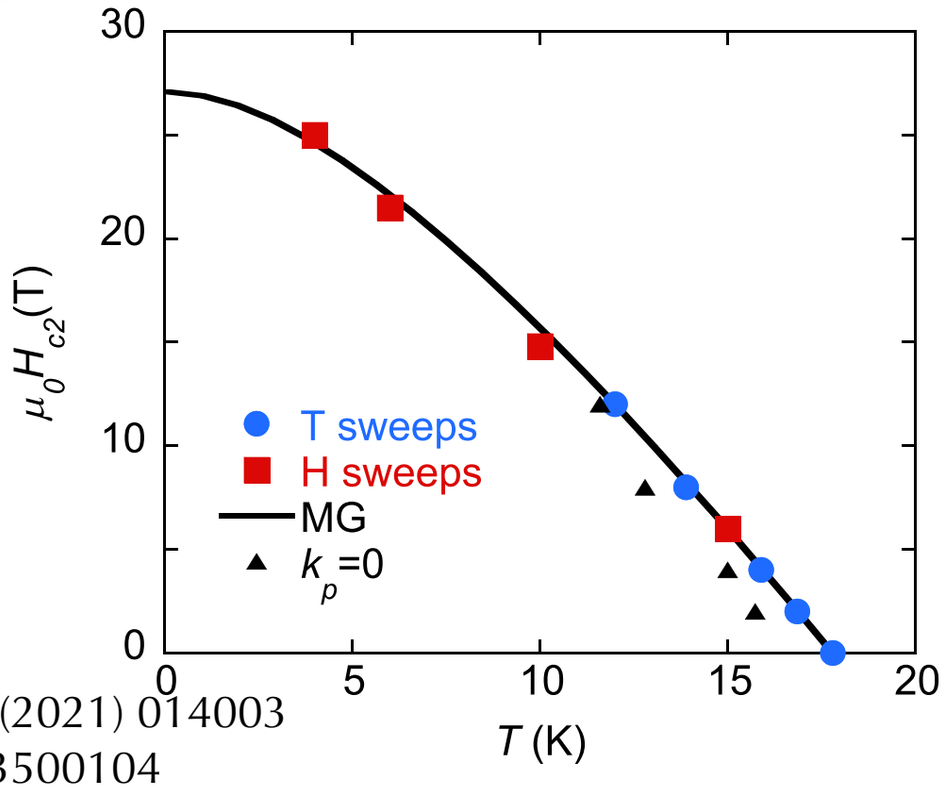

A. Alimenti et al., Supercond. Sci. Technol. 34 (2021) 014003
IEEE Trans. Appl. Supercond. 29 (2019) 3500104

Nb_3Sn: pinning constant

$$Z_S = R_s + iX_s \Rightarrow \rho_1 + i\rho_2 \Rightarrow \quad k_p$$

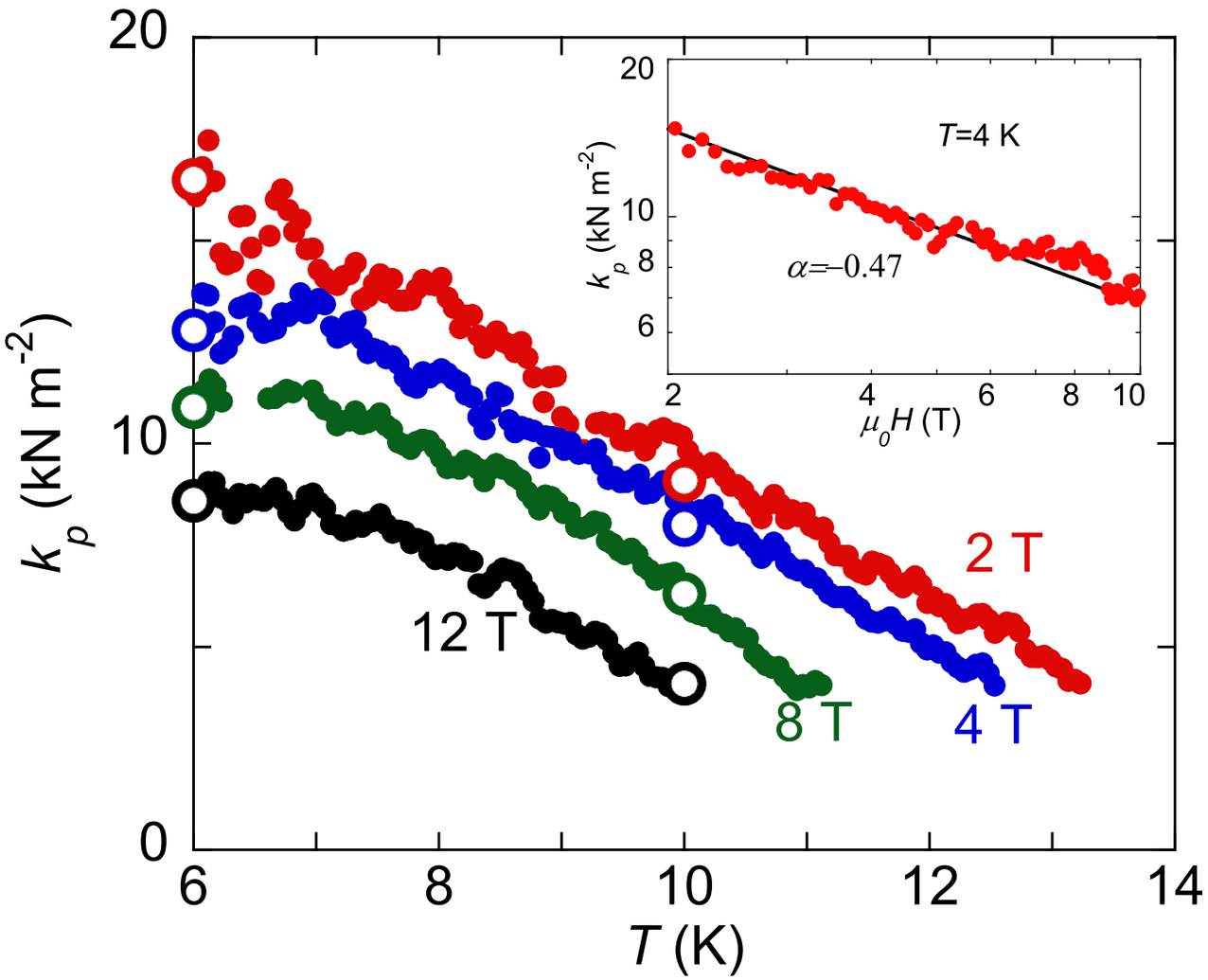

Figure 7. Measured pinning constant $k_p(H, T)$ in FC condition at 2 T, 4 T, 8 T, 12 T. The sparse empty cycles come from the ZFC measurements. In the inset $k_p(H)$ at 4 K is shown in a log-log plot to highlight the power dependence $k_p \propto H^{\alpha}$, with $\alpha = -0.47$, typical of the collective pinning regime.

A. Alimenti et al., Supercond. Sci. Technol. 34 (2021) 014003
IEEE Trans. Appl. Supercond. 29 (2019) 3500104

Nb_3Sn: depinning frequency

$$Z_S = R_s + iX_s \Rightarrow \rho_1 + i\rho_2 \Rightarrow \quad \boldsymbol{\nu_p}$$

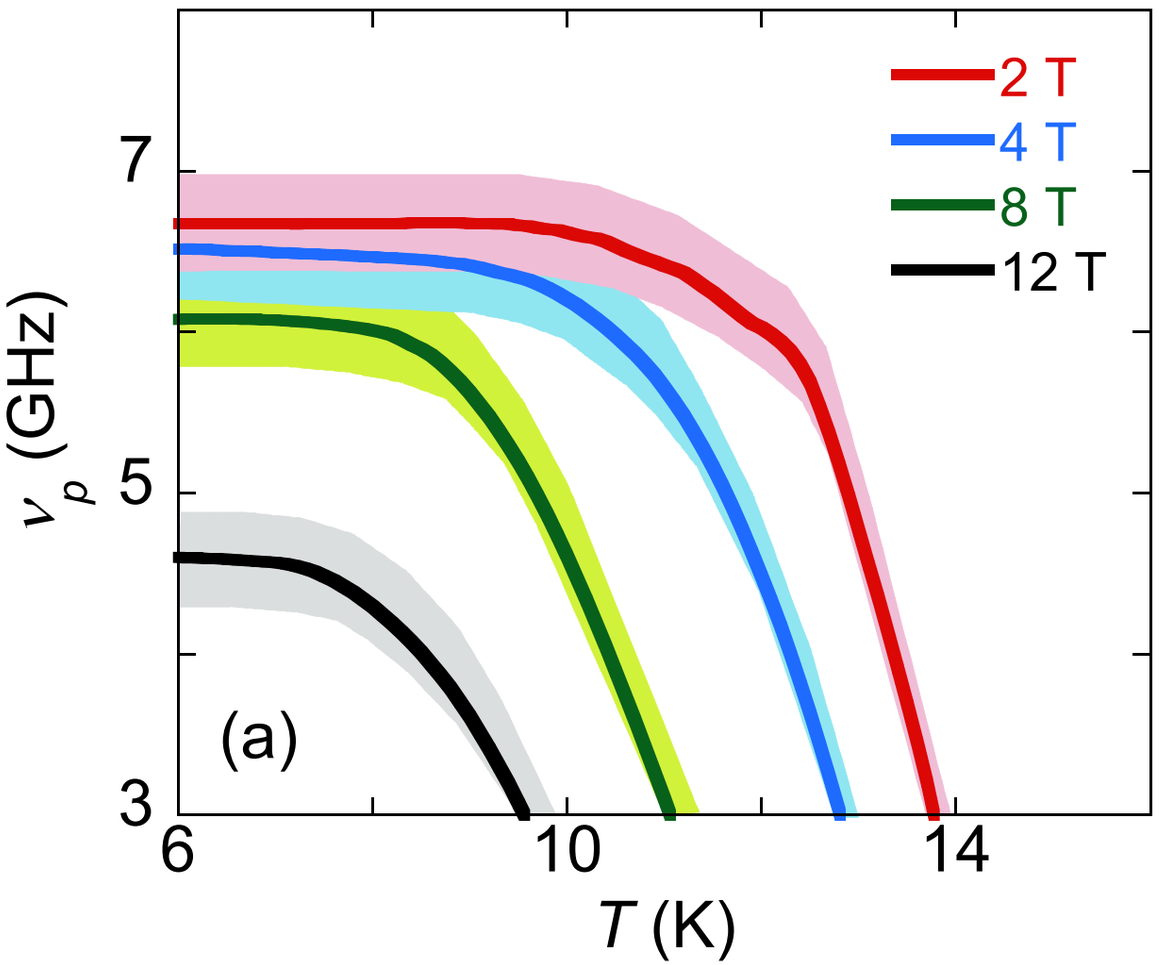

Almost constant at low T
High values (with respect to Nb): potential use for rf applications

Compare to:

Nb *thin films:*

- t = 160 nm $\nu_p \simeq 1$ GHz (T= 0.5 T_c)

D Janjusevic et al, Phys Rev B, **74** 104501 (2006)

YBCO + $BaZrO_3$ *thin films:*

- t = 100 nm $\nu_p \simeq 50$ GHz (T=0.8 T_c)

N. Pompeo et al, APL 91, 182507 2007

YBCO – *coated conductor:*

- t = 175 nm $\nu_p \simeq 70$ GHz (T=77 K)

K Torokhtii et al, IEEE-TAS, **26** 8001605 (2016)
N. Pompeo et al, IEEE-TAS (2019)
DOI: 10.1109/TASC.2019.2897956

A. Alimenti et al., Supercond. Sci. Technol. 34 (2021) 014003
IEEE Trans. Appl. Supercond. 29 (2019) 3500104

$YBa_2Cu_3O_{7-x}/BaZrO_3$

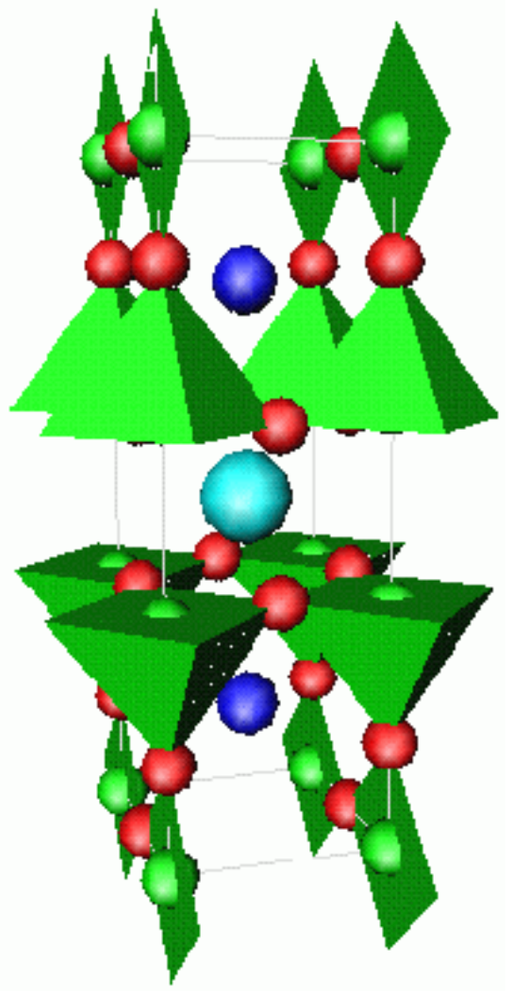

Vortex motion up to high fields

ENEA

Samples:
G. Celentano

YBCO/BZO — Samples

G. Celentano

Thin films YBCO - 5 mol.% BZO sample on $SrTiO_3$ single crystal substrate
grown by chemical deposition
$BaZrO_3$ nanoparticles (Ø~10 nm)

SEM

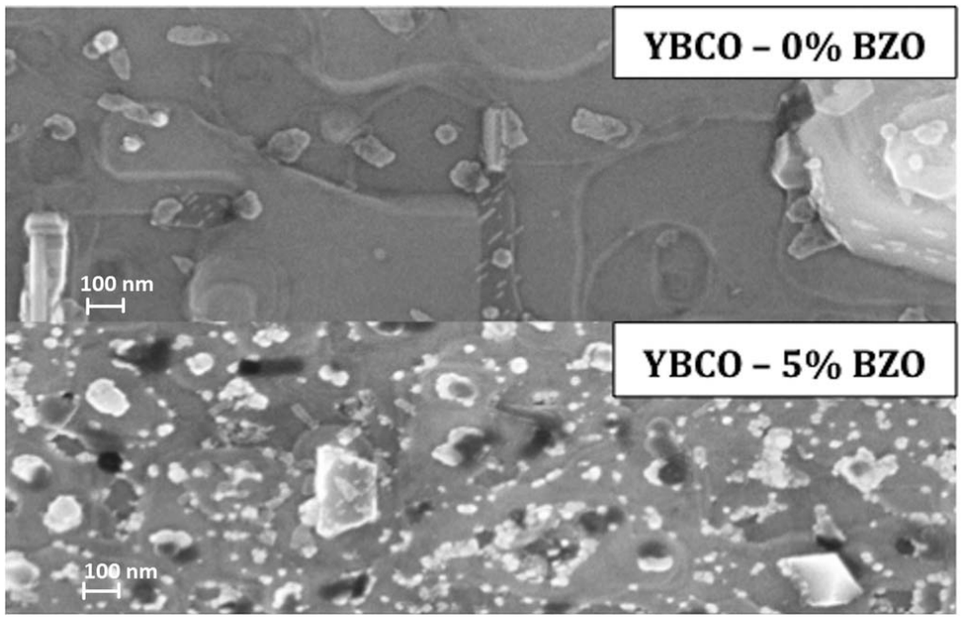

Fig. 1. SEM images of pure YBCO (upper panel) and YBCO/BZO (lower panel) films. The magnification is 100 k × for both images.

A. Frolova et al, IEEE TAS 26, 8001205 (2016)

Critical current density

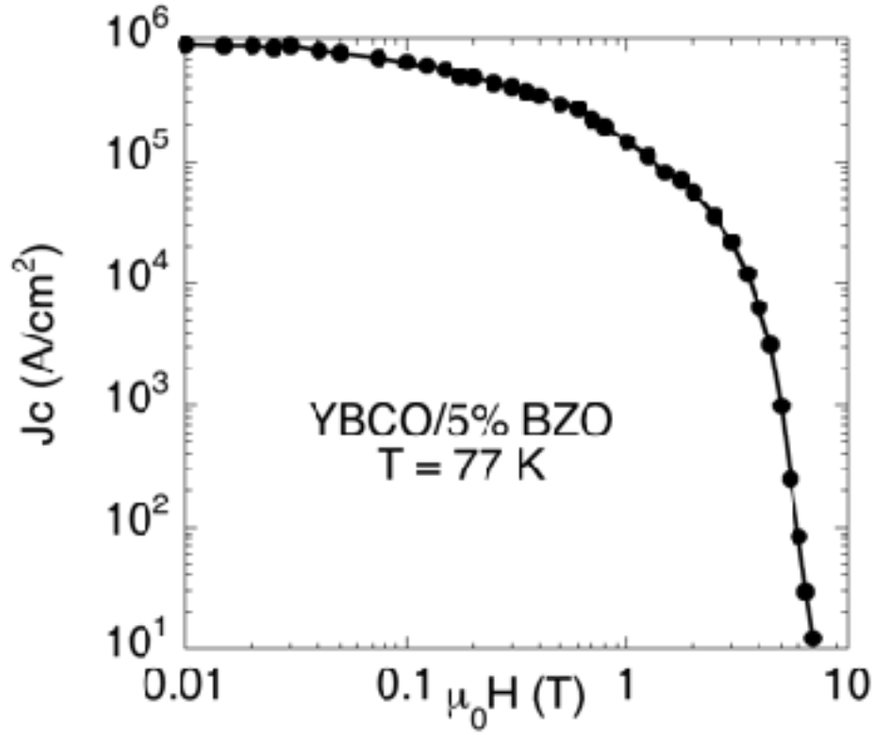

Sharp drop above 1 T
Typical of nanostructured YBCO

YBCO/BZO

field-sweeps: data analysis

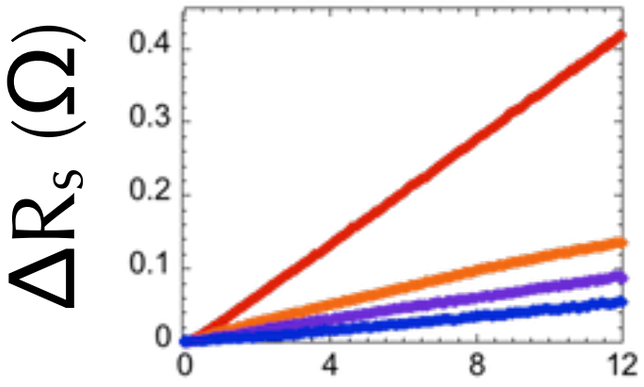

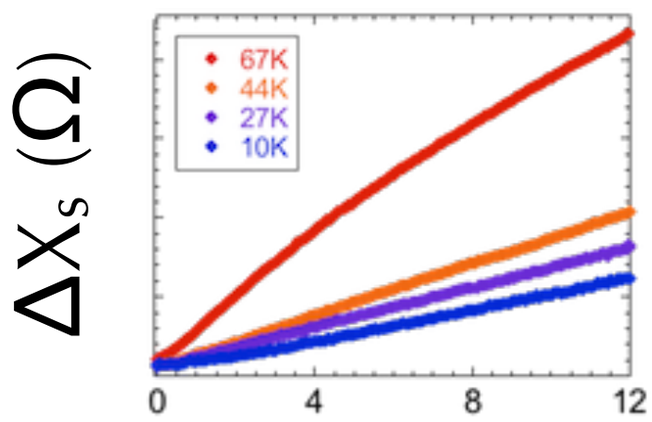

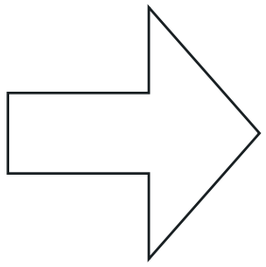

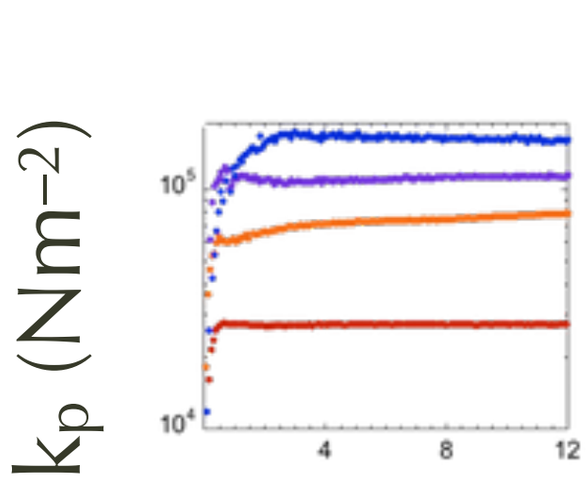

k_p is field-independent up to 12 T:
BZO nanoparticles produce very *steep* potential wells
(height is less efficient: Jc drops)

vs. T

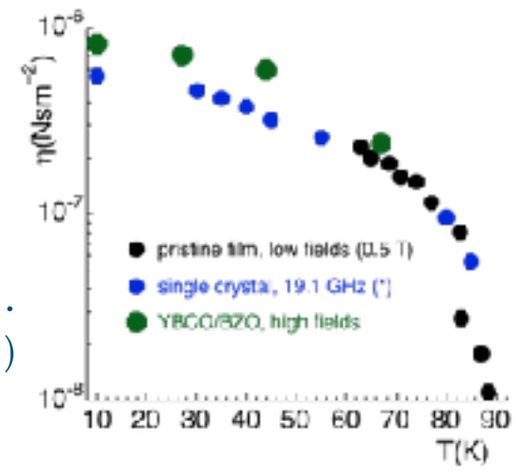

(*) Tsuchiya et al.
PRB 63, 184517 (2001)

Vortex viscosity compares well with data
on single crystals and pristine films:
BZO nanoparticles do not affect the microscopic (quasiparticle) state

high field: YBCO vs. Nb_3Sn

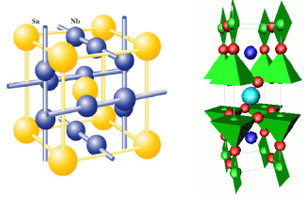

$T/T_c \approx 1/3$

YBCO: 27 K

Nb_3Sn: 6 K

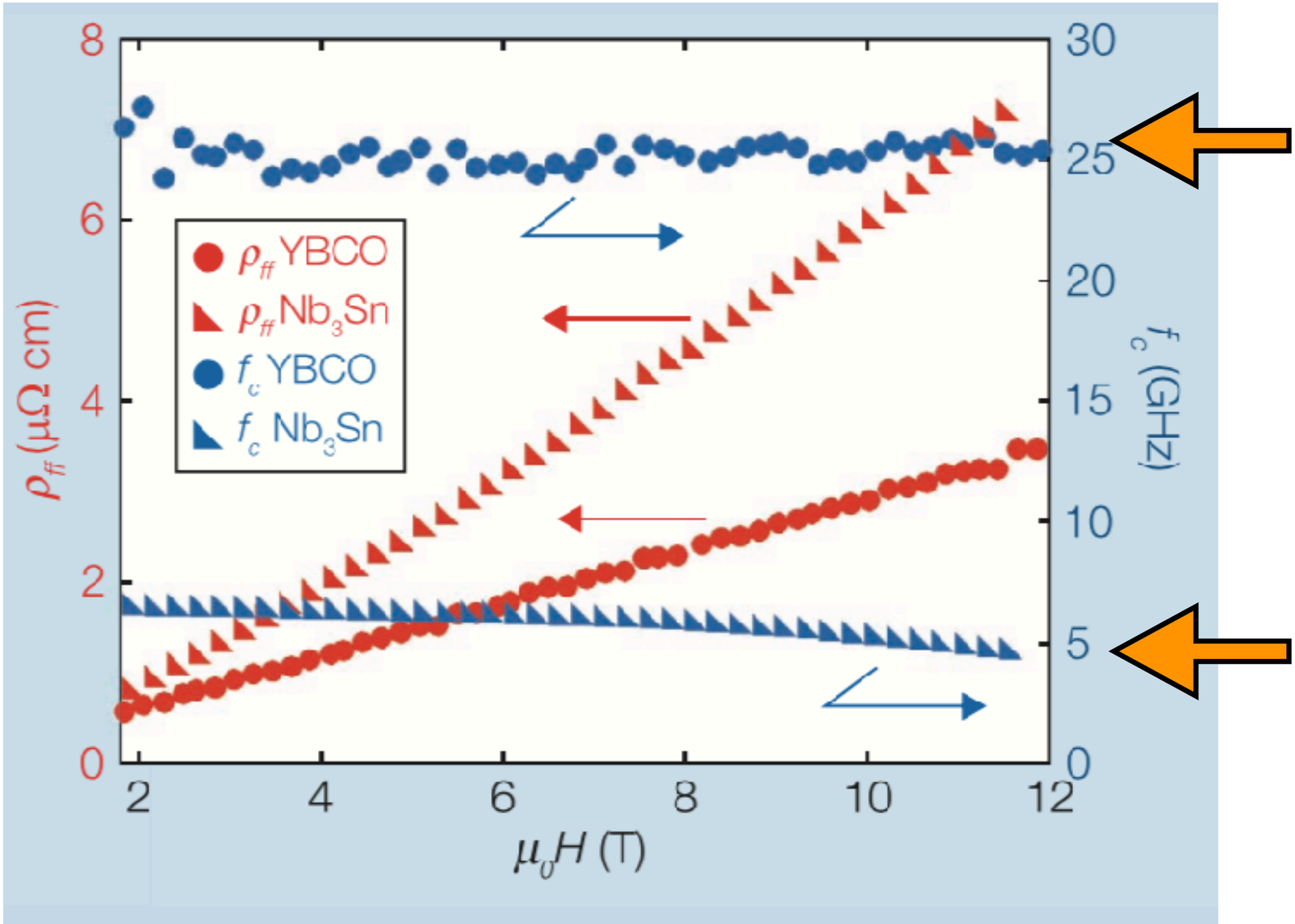

A. Alimenti et al. IEEE Instrum. and Meas. Mag. p.12 (dec. 2021)

N. Pompeo et al., in preparation

Fe(Se,Te)

a new player in the arena?

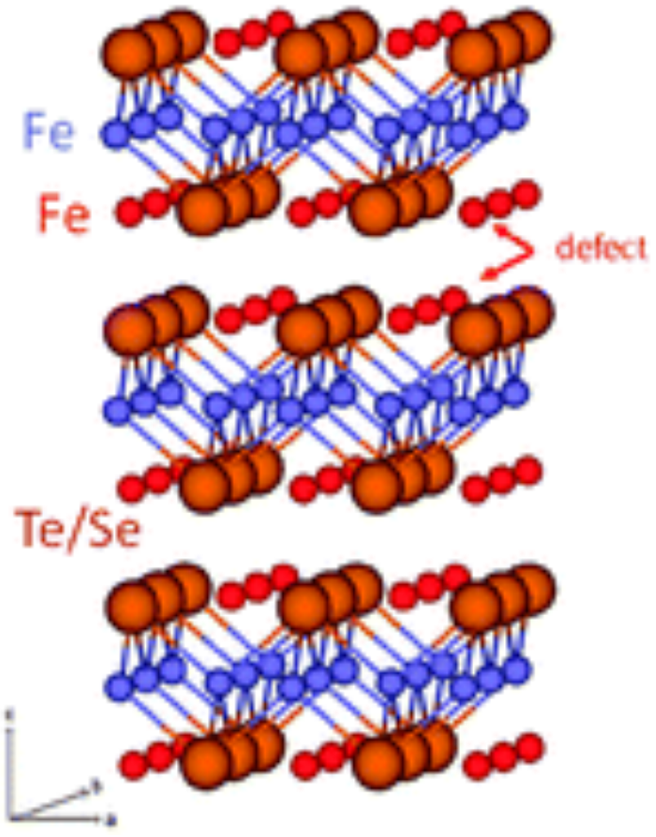

samples: thin films

Samples:
V. Braccini

ROMA TRE
UNIVERSITÀ DEGLI STUDI

Perspectives

rf applications in high fields?

CERN-FCC
Low R_s for wake fields from travelling charged particles. “Beam-screen”

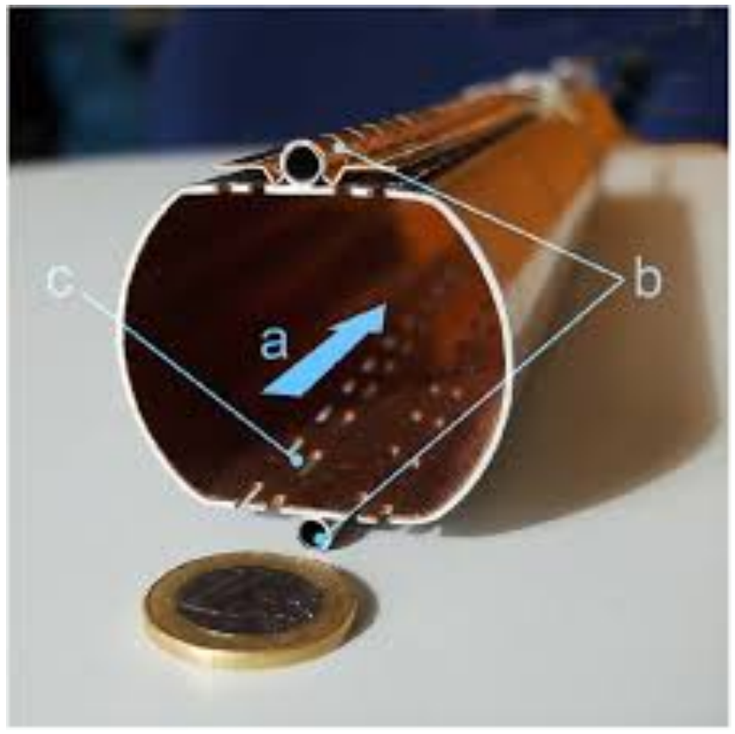

Operates in high-field: 16 T!

Cavity experiments for axion detections

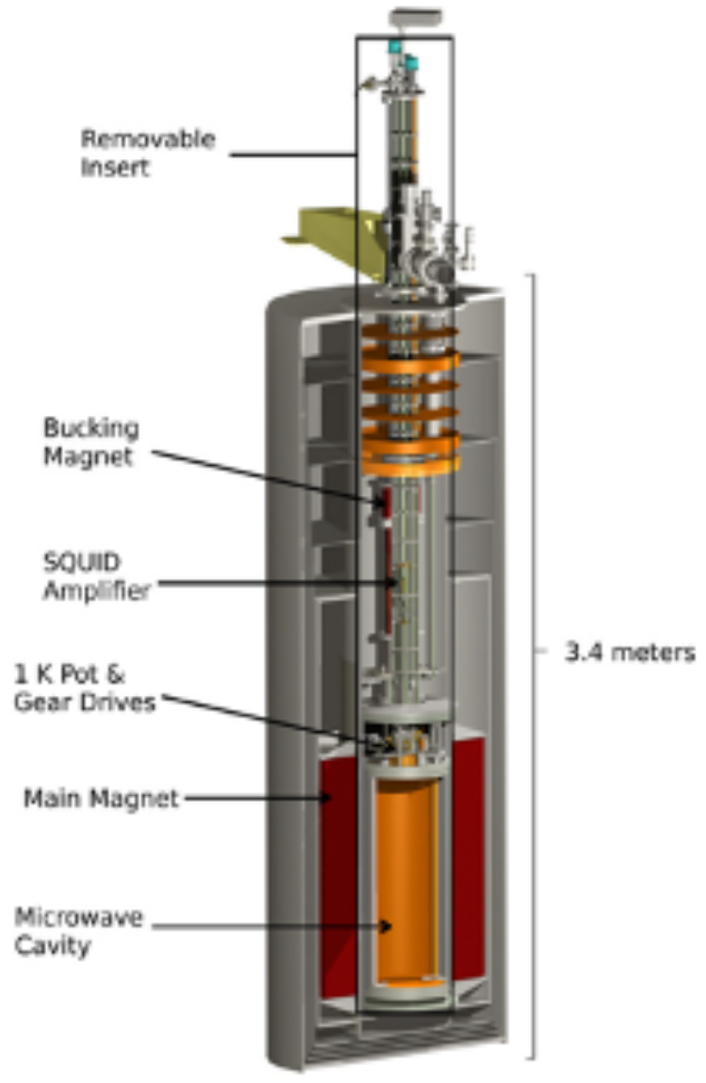

Operates in “moderate”field: 2-8 T

→ high depinning frequency ν_p

Pinning constant k_p

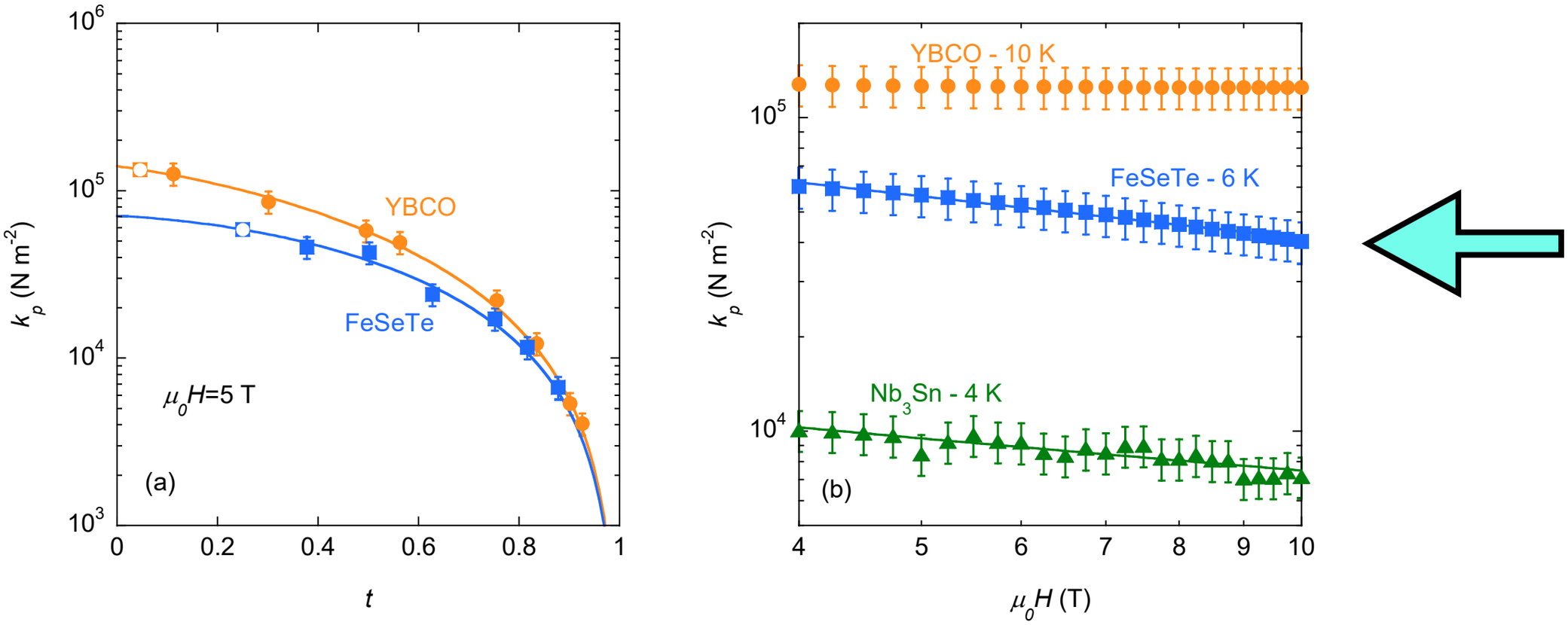

Figure 2. (**a**) Pinning constant k_p, measured on YBCO (orange circles) and FeSeTe (blue squares) in zero field cooling conditions (ZFC) at 5 T as a function of the reduced temperature $t = T/T_c$. The fit of the data is performed with the model developed in [46]: $k_p(t) = k_p(0)(1-t)^{4/3}(1+t)^2 e^{(-T/T_0)}$. The best fit parameters are: $k_p(0) = 1.40 \times 10^5$ N m^{-2} and $T_0 = 56$ K for YBCO, $k_p(0) = 7.07 \times 10^4$ N m^{-2} and $T_0 = T_c$ for FeSeTe. The empty square symbols represent the points extrapolated from the fit at 4 K (which will be used in the next elaborations). (**b**) Field dependence of k_p in Nb_3Sn (green triangle), YBCO, and FeSeTe samples measured at the lower temperatures. $k_p(H)$ in Nb_3Sn and FeSeTe is shown to be $\propto H^{-0.5}$.

A. Alimenti et al., Instruments 6, 1 (2022)

Vortex viscosity η

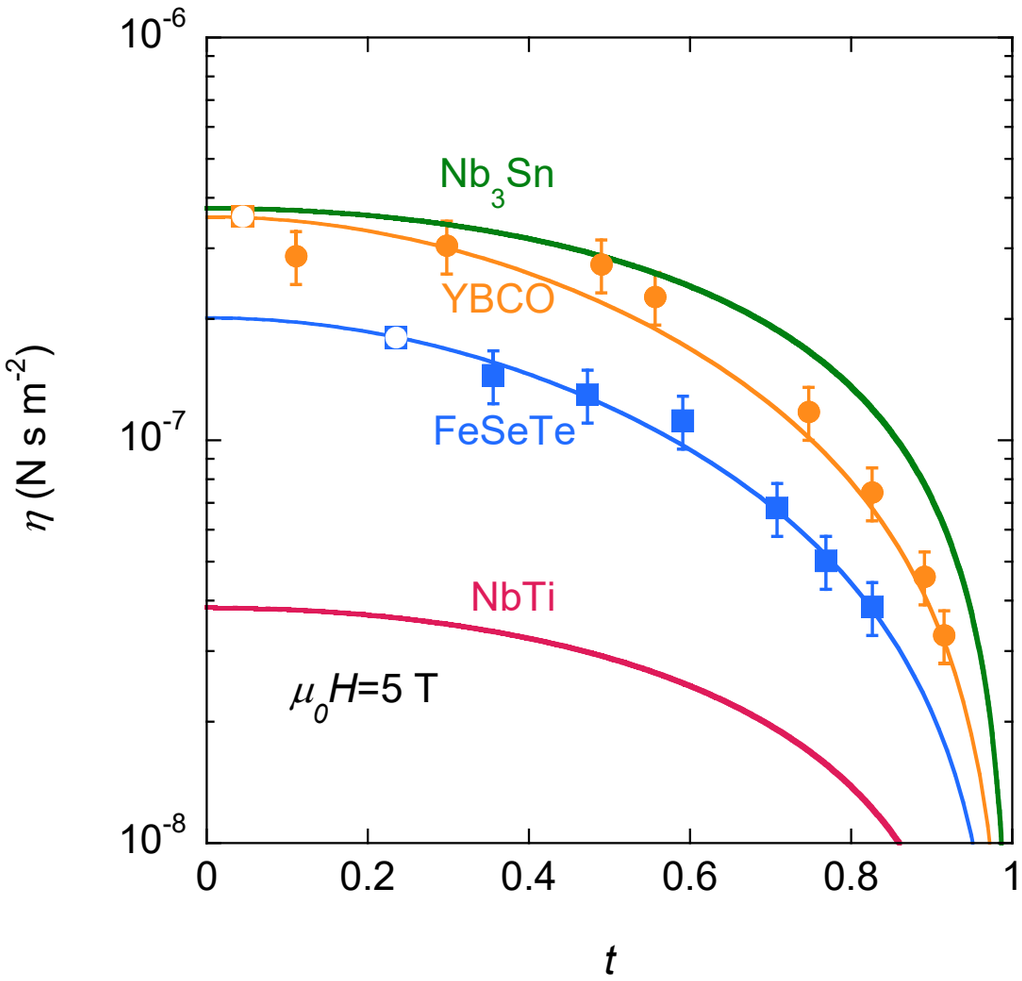

FeSeTe: not too low viscosity

$$\rho_{ff} = \Phi_0 \frac{\mu_0 H}{\eta}$$

Figure 3. Viscous drag coefficient η measured on YBCO (orange circles) and FeSeTe (blue squares) at 5 T in ZFC as a function of the reduced temperature t. The measured data are approximated with $\eta(t) = \eta(0)(1-t^2)/(1+t^2)$ [46], with $\eta(0) = 3.59 \times 10^{-7}$ N s m^{-2} for YBCO and $\eta(0) = 2.02 \times 10^{-7}$ N s m^{-2} for the FeSeTe sample. The empty square symbols represent the points extrapolated from the fit at 4 K (which will be used in the next elaborations). The green and red curves represent $\eta(t)$ obtained by considering $\eta(t) = \Phi_0 B_{c2}(t)/\rho_n$ (from $\rho_{ff} = \rho_n B/B_{c2}$ and $\eta = \Phi_0 B/\rho_{ff}$) for Nb_3Sn and NbTi, respectively.

A. Alimenti et al., Instruments 6, 1 (2022)

parametric plot

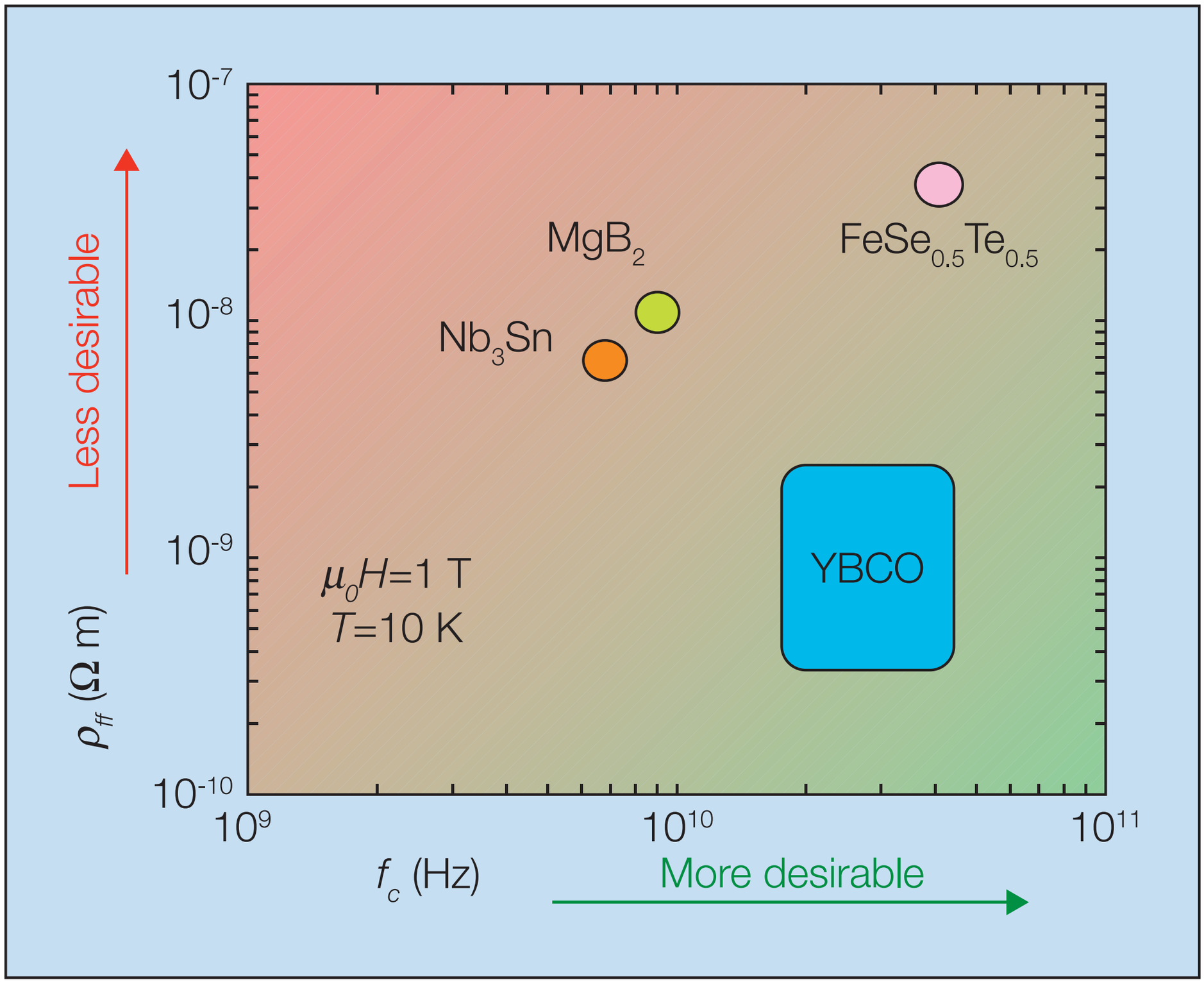

A. Alimenti et al. IEEE Instrum. and Meas. Mag. p.12 (dec. 2021)

comparison

Table 2. Measured parameters of the SCs of interest used for the evaluation of R_s.

	NbTi	**Nb_3Sn**	**YBCO**	**FeSeTe**
k_p (N m^{-2}) at 4 K, 5 T	–	$(9.9 \pm 1.5) \times 10^3$	$(1.3 \pm 0.2) \times 10^5$	$(5.9 \pm 0.9) \times 10^4$
pinning regime	single	collective	single	collective
η (N s m^{-2}) at 4 K, 5 T	–	–	$(3.6 \pm 0.5) \times 10^{-7}$	$(1.8 \pm 0.3) \times 10^{-7}$
ρ_n (μΩ cm)	70 ± 2	14.8 ± 0.2	–	–
$B_{c2}(0)$ (T)	13.0 ± 0.5	27.0 ± 0.5	–	–
ν_p (GHz) at 4 K, 5 T	44 ± 7	4.2 ± 0.6	59 ± 9	52 ± 8
meas. geometry	$\boldsymbol{H} \parallel \boldsymbol{J}$	$\boldsymbol{H} \perp \boldsymbol{J}$	$\boldsymbol{H} \parallel c$ axis, $\boldsymbol{H} \perp \boldsymbol{J}$	
γ	1	1	5.3 ± 0.7	1.8 ± 0.2
$\lambda(0)$ (nm)	270 ± 20 [17,47]	160 ± 20 [48]	150 ± 10 [49,50]	520 ± 50 [45]

optimization of Fe(Se,Te) possible (nanoengineering)!
Maybe better or on par with YBCO,
but good perspectives **for growing as a coating** (at least, FeSe)
(cavity people would be very thankful…)

A. Alimenti et al., Instruments 6, 1 (2022)

Summary

- **Microwaves: a versatile and powerful tool for vortex physics**
- New rf requirements for operation in a dc magnetic field
- Nb_3Sn and YBCO/BZO are mature major players in rf high-field experiments
- FeSeTe: at intrinsic properties level, competitive for rf with Nb_3Sn and, in perspective, with YBCO (but still non mature from material science point of vue)

Thank you for your attention

enrico.silva@uniroma3.it